Supplementary Information for

Norbornene-tetrazine ligation chemistry for controlling RNA-guided CRISPR systems.

Qianqian Qi, Yutong Zhang, Wei Xiong, Xingyu Liu, Shuangyu Cui, Xiaofang Ye, Kaisong Zhang, Tian Tian*, Xiang Zhou

Tian Tian
Email: ttian@whu.edu.cn

This PDF file includes:

Supplementary text

Chemical synthesis.

All reactions in anhydrous solvents were performed in flame-dried glassware under a nitrogen (N_2) atmosphere. Unless otherwise indicated, commercially available reagents were used without further purification. Chromatographic purification was performed on silica gel (100-200 mesh). Analytical thin layer chromatography (TLC) was performed on silica gel 60-F_{254} (Yantai, China) using UV-detection at 230 nm. ^{1}H NMR and ^{13}C NMR were recorded on 400 MHz ^{1}H (101 MHz. ^{13}C) spectrometer in deuterochloroform ($CDCl_3$). The peaks around δ 7.26 (^{1}H NMR) and 77.16 (^{13}C NMR) correspond to $CDCl_3$. Multiplicities are indicated as follows: s (singlet), d (doublet), t (triplet), m (multiplet), dd (doublet of doublets), etc. Coupling constants (*J*) are given in hertz. Chemical shifts (δ) are reported in parts per million relative to TMS as an internal standard. The ESI-HRMS was performed on a Bruker Bio TOF IIIQ (quadrupole time of flight) mass spectrometer.

The NMR spectra of the selected synthesized compounds are given in the appendix sections (**Appendix A**), and HRMS spectra of the tested compounds are also given (**Appendix B**).

The synthesis of NBFI

NBFI (bicyclo[2.2.1]hept-5-en-2-yl 1H-imidazole-1-carboxylate)

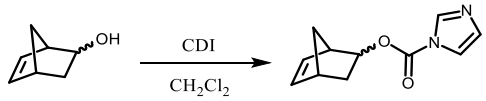

compound **1** **NBFI**

N, *N'*-Carbonyldiimidazole (CDI, 194 mg, 1.2 mmol) was added to a solution of 5-norbornen-2-ol **1** (*endo*/*exo* mixture, 110 mg, 1.0 mmol) in anhydrous CH_2Cl_2 (5 mL). After stirring at room temperature for 2 hr, the mixture was diluted into CH_2Cl_2 (20 mL) and washed with brine (1 × 25 mL). The organic phase was washed with water (2 × 25 mL), dried over anhydrous Na_2SO_4, and concentrated under reduced pressure to obtain the desired product **NBFI** (4:1 *endo*/*exo* mixture, 190 mg, 93%) as a colorless oil which was used without further purification.

^{1}H NMR (400 MHz, $CDCl_3$) δ 8.06-8.04 and 8.14-8.12 (m_{endo}, m_{exo}, 1H), 7.34 and 7.42 (t_{endo}, *J* = 1.4 Hz, t_{exo}, *J* = 1.5 Hz, 1H), 7.05-7.03 and 7.08-7.06, (m_{endo}, m_{exo}, 1H), 6.42 and 6.33 (dd_{endo}, *J* = 5.8, 3.1 Hz, dd_{exo}, *J* = 5.8, 2.9 Hz, 1H), 6.03 ($dd_{endo\ and\ exo}$, *J* = 5.8, 2.8 Hz, 1H), 5.55 and 4.95-4.91 (ddd_{endo}, *J* = 8.2, 3.9, 2.6 Hz, m_{exo}, 1H), 3.32-3.28 and 3.11-3.07 (m_{endo}, m_{exo}, 1H), 2.98-2.91 ($m_{endo\ and\ exo}$, 1H), 2.27 and 1.87 (ddd_{endo}, *J* = 12.8, 8.1, 3.7 Hz, ddd_{exo}, *J* = 12.9, 6.9, 2.3 Hz, 1H), 1.65-1.55 ($m_{endo\ and\ exo}$, 1H), 1.75-1.68 and 1.43-1.39 (m_{exo}, m_{endo}, 1H), 1.75-1.68 and 1.13 (m_{exo}, ddd_{endo}, *J* = 12.8, 3.8, 2.6 Hz, 1H).

^{13}C NMR (101 MHz, $CDCl_3$) δ 148.62, 148.58, 141.87, 139.32, 137.03, 137.00, 131.94, 130.92, 130.57, 130.50, 117.08, 117.02, 79.87, 79.45, 47.74, 47.33, 46.34, 45.88, 42.25, 40.59, 34.62, 34.60.

HRMS (ESI^+) m/z calcd for $C_{11}H_{13}N_2O_2$ $[M + H]^+$: 205.0972, found: 205.0976.

Synthesis of 6-(6-(pyrimidin-2-yl)-1,2,4,5-tetrazin-3-yl)nicotinic acid (sTz) (1, 2)

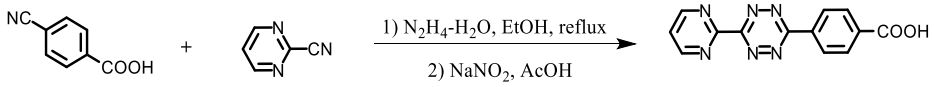

compound **2** compound **3** ***s*-Tz**

4-Cyanobenzoic acid (compound **2**, 7.06 g, 48 mmol) and 2-cyanopyrimidine (compound **3**, 5.04 g, 48 mmol) were suspended in dry EtOH (30 mL) under nitrogen atmosphere and hydrazine monohydrate (12 g, 240 mmol) was added dropwise by syringe at room temperature. The resulting mixture was vigorously stirred at 90 °C for 12 hr. After cooling to room temperature, the orange precipitate was filtered off and washed with cold EtOH. The solid was stirred in refluxing acetone (50 mL) and filtered off in the heat to remove the byproduct. The orange solid was suspended in acetic acid (100 mL) and $NaNO_2$ (3.31 g, 48 mmol) in water (50 mL) was added dropwise at 0 °C. The resulting mixture was vigorously stirred for 3 h and the precipitate was filtered off and washed with water (1 × 100 mL) and cold EtOH (1 × 20 mL). Then, the solid was dried under reduced pressure to afford a purple solid ***s*-Tz** (2.42 g, 18%).

^{1}H NMR ^{1}H NMR (400 MHz, DMSO-*d*6) δ 13.40 (s, 1H), 9.21 (d, *J* = 4.9 Hz, 2H), 8.71 (d, *J* = 8.4 Hz, 2H), 8.26 (d, *J* = 8.4 Hz, 2H), 7.85 (t, *J* = 4.9 Hz, 1H).

^{13}C NMR (101 MHz, DMSO-d_6) δ 166.23, 162.71, 162.45, 158.57, 158.08, 134.90, 134.00, 129.81, 127.90, 122.59.

HRMS (ESI$^+$) m/z calcd for $C_{13}H_9N_6O_2$ [M + H] $^+$: 281.0781, found: 281.0790.

Synthesis of 2,5-dioxopyrrolidin-1-yl 4-(6-(pyrimidin-2-yl)-1,2,4,5-tetrazin-3-yl)benzoate

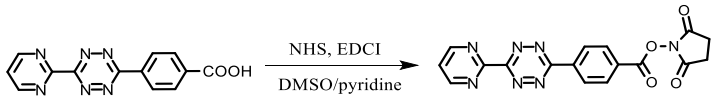

***s*-TZ** compound **4**

s-TZ (1.68 g, 6 mmol), N-hydroxysuccinimide (NHS, 1.03 g, 9 mmol), and 1-ethyl-3-(3-dimethylaminopropyl)carbodiimide hydrochloride (EDCI, 1.72 g, 9 mmol) were dissolved in DMSO/pyridine (22:3, 25 mL). The resulting mixture was stirred at 40 °C for 2 hr, then the reaction was diluted with CH_2Cl_2 (200 mL) and washed with water (2 × 200 mL) and brine (1 × 200 mL). The organic layer was dried over anhydrous Na_2SO_4, filtered and the solvent was removed under reduced pressure. The crude product was purified by silica gel column chromatography (CH_2Cl_2/EtOAc)to afford compound **4** (1.81 g, 80%) as a purple solid.

^{1}H NMR (400 MHz, DMSO-d_6) δ 9.23 (d, J = 4.9 Hz, 2H), 8.89-8.83 (m, 2H), 8.47-8.40 (m, 2H), 7.87 (t, J = 4.9 Hz, 1H), 2.95 (s, 4H).

^{13}C NMR (101 MHz, DMSO-d_6) δ 170.72, 163.39, 161.86, 159.44, 159.06, 138.21, 131.51, 129.53, 128.35, 123.60, 26.07.

HRMS (ESI$^+$) m/z calcd for $C_{17}H_{12}N_7O_4$ [M + H] $^+$: 378.0945, found: 378.0954.

Synthesis of *N*,*N*'-(((oxybis(ethane-2,1-diyl))bis(oxy))bis(ethane-2,1-diyl))bis(4-(6-(pyrimidin-2-yl)-1,2,4,5-tetrazin-3-yl)benzamide) (*d*-TZ)

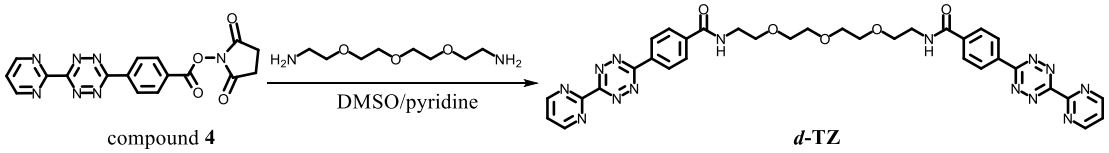

compound **4** ***d*-TZ**

The active ester **4** (415 mg, 1.1 mmol) and 3,6,9-trioxaundecane-1,11-diamine (96 mg, 0.5 mmol) were dissolved in dry DMSO/pyridine (9:1, 10 mL). The resulting mixture was stirred at 50 °C for 12 hr. After cooling to room temperature, the solvent was removed under vacuum and the residue was redissolved in CH_2Cl_2. The organic layer was washed with water and brine, dried over anhydrous Na_2SO_4, filtrated and the solvent was evaporated under reduced pressure. The crude product was purified by silica gel column chromatography (CH_2Cl_2/MeOH) to afford compound ***d*-Tz** (**7**, 630 mg, 88%) as a purple solid.

^{1}H NMR (400 MHz, $CDCl_3$) δ 9.14 (d, J = 4.9 Hz, 4H), 8.78 (d, J = 8.1 Hz, 4H), 8.06 (d, J = 8.1 Hz, 4H), 7.61 (t, J = 4.9 Hz, 2H), 7.06 (br, 2H), 3.66-3.74 (m, 16H).

^{13}C NMR (101 MHz, $CDCl_3$) δ 166.50, 164.02, 163.18, 159.44, 158.46, 138.76, 133.83, 128.89, 128.12, 122.60, 70.53, 70.25, 69.72, 39.96.

HRMS (ESI$^+$) m/z calcd for $C_{34}H_{33}N_{14}O_5$ [M + H] $^+$: 717.2753, found: 717.2767.

HRMS (ESI$^+$) m/z calcd for $C_{34}H_{32}N_{14}NaO_5$ [M + Na] $^+$: 739.2572, found: 739.2586.

Synthesis of *N*,*N*',*N*''-(nitrilotris(ethane-2,1-diyl))tris(4-(6-(pyrimidin-2-yl)-1,2,4,5-tetrazin-3-yl)benzamide)

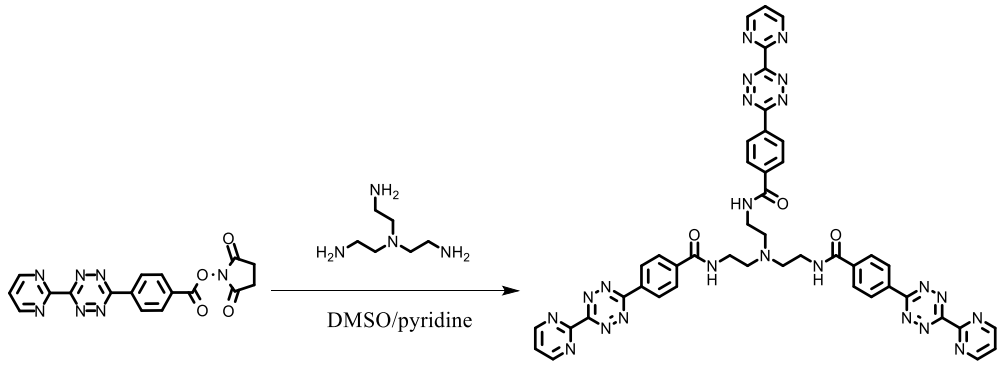

compound **4** ***t*-TZ**

The active ester **4** (415 mg, 1.1 mmol) and tris(2-aminoethyl)amine (48 mg, 0.33 mmol) were dissolved in dry DMSO/pyridine (9:1, 10 mL). The resulting mixture was stirred at 50 °C for 12 hr. After cooling to room temperature, the solvent was removed under vacuum and the residue was redissolved in CH_2Cl_2. The organic layer was washed with water and brine, dried over anhydrous Na_2SO_4, filtrated and the solvent was evaporated under reduced pressure. The crude product was purified by silica gel column chromatography (CH_2Cl_2/MeOH) to afford ***t*-Tz** (**8**, 249 mg, 81%) as a purple solid.
^{1}H NMR (400 MHz, DMSO-d_6) δ 9.04 (d, J = 4.9 Hz, 6H), 8.54 (t, J = 5.5 Hz, 3H), 8.43 (d, J = 8.2 Hz, 6H), 8.03 (d, J = 8.2 Hz, 6H), 7.75 (t, J = 4.9 Hz, 3H), 3.53 (q, J = 6.0 Hz, 6H), 2.85 (t, J = 6.3 Hz, 6H).
^{13}C NMR (101 MHz, DMSO-d_6) δ 166.10, 163.44, 163.22, 159.35, 158.75, 138.55, 134.11, 128.58, 128.40, 123.29, 52.93, 37.85.
HRMS (ESI$^+$) m/z calcd for $C_{45}H_{37}N_{22}O_3$ [M + H] $^+$: 933.3413, found: 933.3432.
HRMS (ESI$^+$) m/z calcd for $C_{45}H_{36}N_{22}NaO_3$ [M + Na] $^+$: 955.3233, found: 955.3251.

Synthesis of *N*,*N*',*N*'',*N*'''-((ethane-1,2-diylbis(azanetriyl))tetrakis(ethane-2,1-diyl))tetrakis(4-(6-(pyrimidin-2-yl)-1,2,4,5-tetrazin-3-yl)benzamide)
Tetra-tert-butyl ((ethane-1,2-diylbis(azanetriyl))tetrakis(ethane-2,1-diyl))tetracarbamate

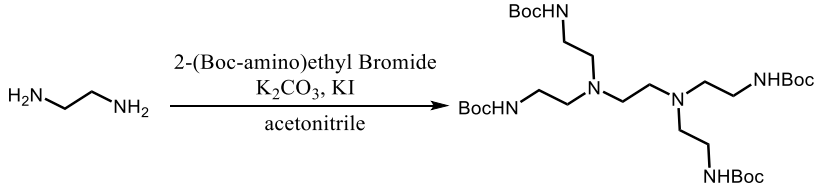

compound **5** compound **6**

Ethylenediamine (compound **5**, 601 mg, 10 mmol), anhydrous K_2CO_3 (6.2 g, 45 mmol), and KI (664 mg, 4.0 mmol) were added in acetonitrile (100 mL). 2-(Boc-amino)ethyl bromide (10 g, 45 mmol) in acetonitrile (20 mL) was added slowly by syringe at 0 °C under nitrogen atmosphere, and the resulting mixture was stirred vigorously at room temperature for 60 hr. The solid was filtered and the filtrate was concentrated under reduced pressure to give a colorless oil which was purified by silica gel column chromatography (CH_2Cl_2/MeOH /NH_3 (7.0 M solution in MeOH)) to afford compound **6** as a colorless oil (3.3 g, 52%).
^{1}H NMR (400 MHz, $CDCl_3$) δ 4.49-4.45 (m, 2H), 3.65 (td, J = 7.8, 0.9 Hz, 2H), 3.15-3.22 (m, 6H), 2.60-2.51 (m, 10H), 1.45 (s, 36H).
^{13}C NMR (101 MHz, $CDCl_3$) δ 156.17, 79.23, 64.92, 53.76, 40.52, 28.47.
HRMS (ESI$^+$) m/z calcd for $C_{30}H_{61}N_6O_8$ [M + H] $^+$: 633.4545, found: 633.4549.

***N*^{1},*N*$^{1'}$-(ethane-1,2-diyl)bis(*N*^{1}-(2-aminoethyl)ethane-1,2-diamine) hexahydrochloride**

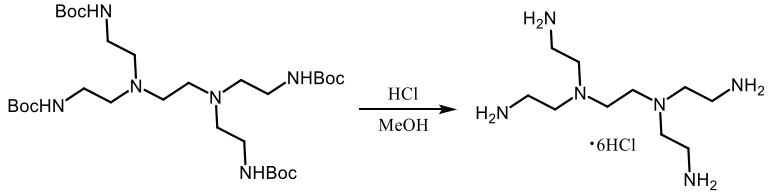

compound **6** compound **7**

Compound **6** (1.9 g, 3 mmol) was dissolved in MeOH (10 mL) and 12 M HCl (20 mL) was added slowly at 0 °C in one portion. The resulting mixture was heated to 50 °C for 2 hr and the solvent was removed under reduced pressure to give an off-white solid which was washed with EtOH to afford product **7** as a white solid (3.3 g, 96%).
^{1}H NMR (400 MHz, D_2O) δ 3.25 (dd, J = 7.6, 5.6 Hz, 8H), 3.20-3.11 (m, 12H).
^{13}C NMR (101 MHz, D_2O) δ 49.91, 49.00, 35.28.
HRMS (ESI$^+$) m/z calcd for $C_{10}H_{29}N_6$ [M + H] $^+$: 233.2448, found: 233.2446.

***N*,*N*',*N*'',*N*'''-((ethane-1,2-diylbis(azanetriyl))tetrakis(ethane-2,1-diyl))tetrakis(4-(6-(pyrimidin-2-yl)-1,2,4,5-tetrazin-3-yl)benzamide)**

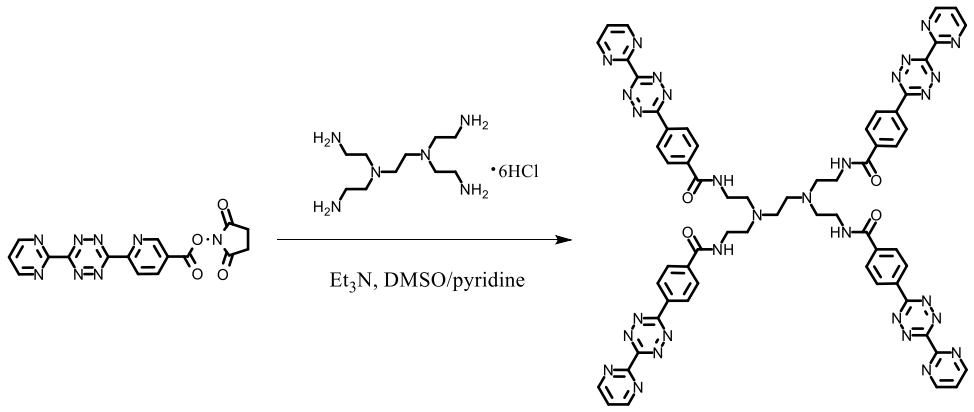

compound **4** ***q*-TZ**

The active ester **4** (415 mg, 1.1 mmol) and N^1,$N^{1'}$-(ethane-1,2-diyl)bis(N^1-(2-aminoethyl)ethane-1,2-diamine) hexahydrochloride **7** (113 mg, 0.25 mmol) were dissolved in dry DMSO/pyridine/Et_3N (8.5:1:0.5, 10 mL). The resulting mixture was stirred at 50 °C for 12 hr. After cooling to room temperature, the solvent was removed under vacuum and the residue was redissolved in CH_2Cl_2. The organic layer was washed with water, dried over Na_2SO_4, filtrated and the solvent was removed under reduced pressure. The crude product was purified by silica gel column chromatography (CH_2Cl_2/MeOH) to afford ***q*-Tz** (227 mg, 72%) as a purple solid.

^{1}H NMR (400 MHz, DMSO-d_6) δ 9.11 (d, J = 4.9 Hz, 8H), 8.60 (t, J = 5.4 Hz, 4H), 8.56-8.52 (m, 8H), 8.10-8.05 (m, 8H), 7.78 (t, J = 4.9 Hz, 4H), 3.48 (q, J = 6.3 Hz, 8H), 2.84-2.72 (m, 12H).

^{13}C NMR (101 MHz, DMSO-d_6) δ 165.99, 163.52, 163.27, 159.39, 158.86, 138.76, 134.09, 128.61, 128.50, 123.37, 53.60, 52.39, 38.14.

HRMS (ESI^+) m/z calcd for $C_{62}H_{53}N_{30}O_4$ $[M + H]^+$: 1280.4861, found: 1280.4876.

General methods of biological assay

Materials

All oligonucleotide sequences are provided in Table S1. The oligonucleotides were synthesized from TaKaRa company (Dalian, China). RNA concentration was expressed in strand molarity using a nearest-neighbor approximation for the extinction coefficients of the unfolded species. The Cas9 Nuclease, *Streptococcus pyogenes* (product# M0646), the ribonucleotide solution mix (NTPs) and deoxy-ribonucleoside triphosphates (dNTPs) were purchased from New England Biolabs, Inc. (USA). All chemicals were purchased from Sigma-Aldrich (Shanghai, China). The nucleic acid stains Super GelRed (NO.: S-2001) was purchased from US Everbright Inc. (Suzhou, China). The Pyrobest™ DNA Polymerase were purchased from TaKaRa Shuzo Co. Ltd. (Tokyo, Japan). Transcript Aid T7 High Yield Transcription kit (product# K0441) and Glycogen (product# R0561) were purchased from Thermo Fisher Scientific. The DNA Clean & Concentrator™-5 kit (product# D4014) was purchased from Zymo Research Corp. The pH was measured with Mettler Toledo, FE20-Five Easy™ pH (Mettler Toledo, Switzerland). The concentration of nucleic acids was quantified by NanoDrop 2000c (Thermo Scientific, USA). UV melting experiments were performed on a Jasco-810 spectropolarimeter (Jasco, Easton, MD, USA) equipped with a Peltier temperature controller.

***In vitro* transcription and purification of long RNAs**

In vitro transcription with the T7 RNA polymerase is performed to synthesize the Pepper RNAs and various gRNAs. To generate the target-coding template, we designed separate shorter overlapping sequences(3). Transcription reactions were performed at 37 ℃ for 4.0 hr using a HiScibe T7 quick high yield RNA synthesis kit (NEB). Following DNA degradation using DNase I at the end of the transcription, the transcribed RNA products were then purified using the NaOAc/phenol/chloroform method. The purified RNA was quantified by spectrometry and stored at - 80 °C.

Cell culture

HEK293T, HeLa cells were obtained from ATCC (the American Type Culture Collection). Human HeLa-OC cell line was a kind gift from Prof. Wen-Sheng Wei, Biodynamic Optical Imaging Center (BIOPIC),

School of Life Sciences, Peking University, Beijing, China. HEK293T, HeLa and HeLa-OC cells were cultured in Dulbecco's Modified Eagle Medium (DMEM) with high glucose, containing 10% fetal bovine serum (FBS, Thermo Fisher Scientific), L-glutamine (2 mM), penicillin (100 units/ml) and streptomycin (100 μg/ml), incubated at 37 °C in a humidified atmosphere of 5% CO_2 and 95% air.

Cell survival assay

HeLa or HeLa-OC cells (5×10^4) were seeded into wells of a 96-well plate and incubated for 16 hr. Then cells were treated with different concentrations of freshly dissolved *t*-TZ or DMSO control for 24 hr. After centrifugation at 2000 rpm for 10 min, the medium was discarded and fresh medium was added. Subsequently, the 3-(4,5-dimethylthiazol-2-yl)-2,5-diphenyltetrazolium bromide (MTT) (20 μL, 5 mg/mL in DMSO) was added to each well and the mixture was incubated for an additional 4 hr. After centrifugation at 2000 rpm for 10 min, the medium was removed. Subsequently, DMSO (150 μL) was added to each well and the OD values at 570 nm were detected by a microplate reader (SpectraMax M5, Molecular Devices) to evaluate cell viability. Values were plotted relative to the mean of DMEM control set to 100% (= relative growth). All data were presented as the means ± SEM from three independent experiments.

Cas13a expression and purification

The LbuCas13a plasmid (#83482) was purchased from Addgene(4). This plasmid was transformed into *E. coli* BL21 (DE3) cells. Single colonies were picked and grown in LB media supplemented with 50 μg/mL Ampicillin. Culture was grown to an OD_{600} of 0.5. Protein expression was induced with 0.2 mM isopropyl-β-D-thiogalactopyranoside (IPTG) at 16 °C for 16 hr. Cells from 2-L culture were pelleted by centrifugation at 6000 *g* at 4 °C for 15 min and then re-suspended in 40 mL binding buffer containing 50 mM Na_3PO_4, pH 7.0, and 0.3 M NaCl. Cells were lysed by sonication on ice. Upon centrifugation, the supernatant of cell lysate was incubated with Ni Sepharose (GE Healthcare) at 4 °C for 1 hr, and the bound protein was eluted with 5 mL elute buffer that was made by supplementing binding buffer with 100 mM imidazole. The His6-MBP tag of eluted proteins were removed by TEV protease digestion. Target proteins were purified on an SP column (GE Healthcare), eluting with a buffer (20 mM Tris-HCl, 1M NaCl, pH 7.5). Target proteins were further purified by gel filtration using Superose 6 10/300 column (GE Healthcare). These proteins were buffer-exchanged to storage buffer containing 20 mM Tris-HCl, 100 mM NaCl, pH 7.5, aliquoted and stored at - 80 °C.

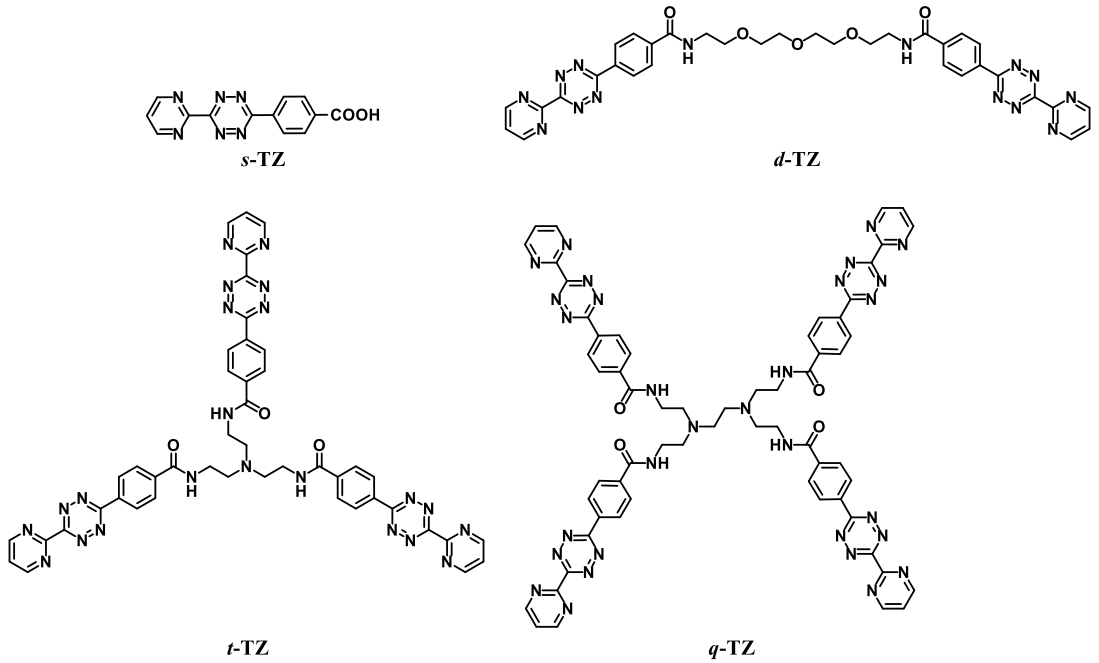

Figure S1. Structures of TZ derivatives in this study.

A variety of TZ derivatives are designed and synthesized to develop clickable RNA switches. All of these TZ derivatives were well characterized by spectroscopic techniques such as ^{1}H NMR, ^{13}C NMR and mass spectrometry. All of these molecules showed excellent solubility due to the introduction of hydrophilic chains, making them useful for biological study without significant aggregation (facilitating their reaction with NB-bearing RNAs).

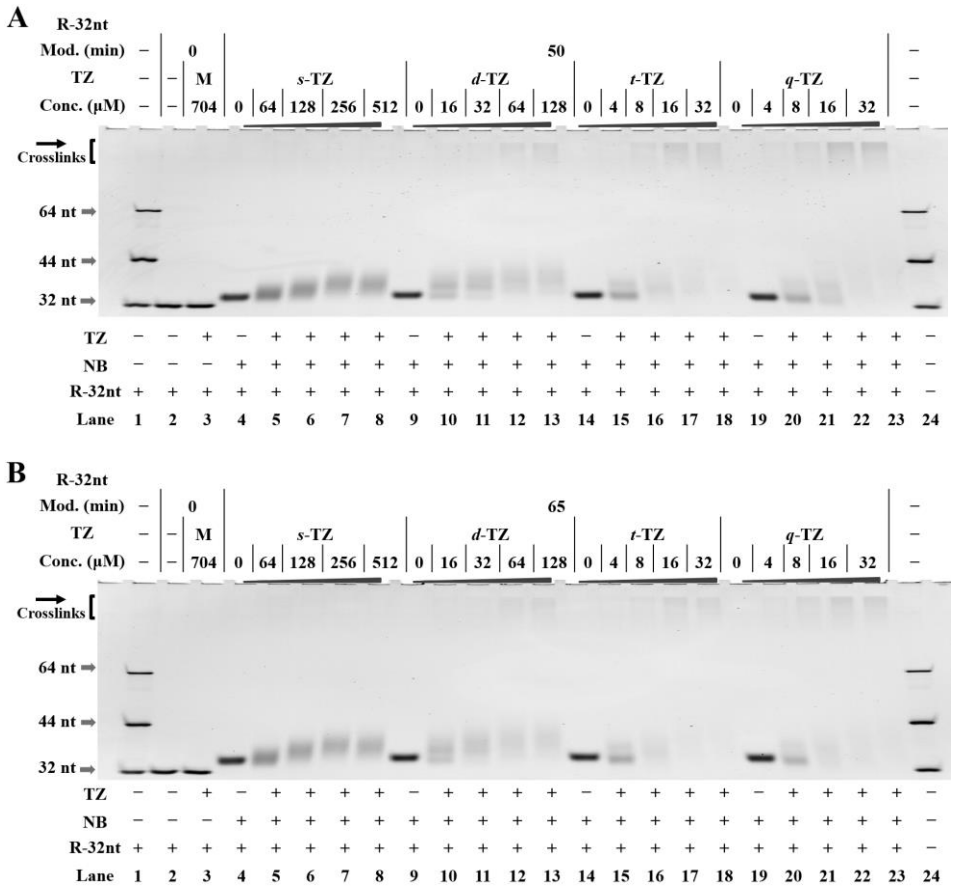

Figure S2. Gel electrophoretic characterization of RNA-based NB-TZ ligation chemistry (R-32nt).

Reactions were performed as described in the Experimental Section. The treatment for each sample is indicated by the signs at the bottom of each lane. All samples were tested in three biological replicates. Image of representative data is shown here. The movement of RNAs is evidently impeded with NB-TZ ligation chemistry and this effect became more evident with increasing concentration of each TZ. In contrast to *s*-TZ, multimeric TZ derivatives are efficient to crosslink NB-bearing RNAs. For the TZ treatment, the capital letter M indicates the cotreatment with *s*-TZ (512 μM), *d*-TZ (128 μM), *t*-TZ (32 μM) and *q*-TZ (32 μM). (**A**) Lanes 1, 24: RNA marker (R-32nt, R-44nt, R-64nt in Table S1); lanes 2-3 contain native R-32nt; lanes 4-8, 9-13, 14-18, 19-23 contain NB-bearing R-32nt with a specified level of modification (a 50-min modification with 20 mM NBFI). (**B**) Lanes 1, 24: RNA marker (R-32nt, R-44nt, R-64nt); lanes 2-3 contain native R-32nt; lanes 4-8, 9-13, 14-18, 19-23 contain NB-bearing R-32nt with a specified level of modification (a 65-min modification with 20 mM NBFI).

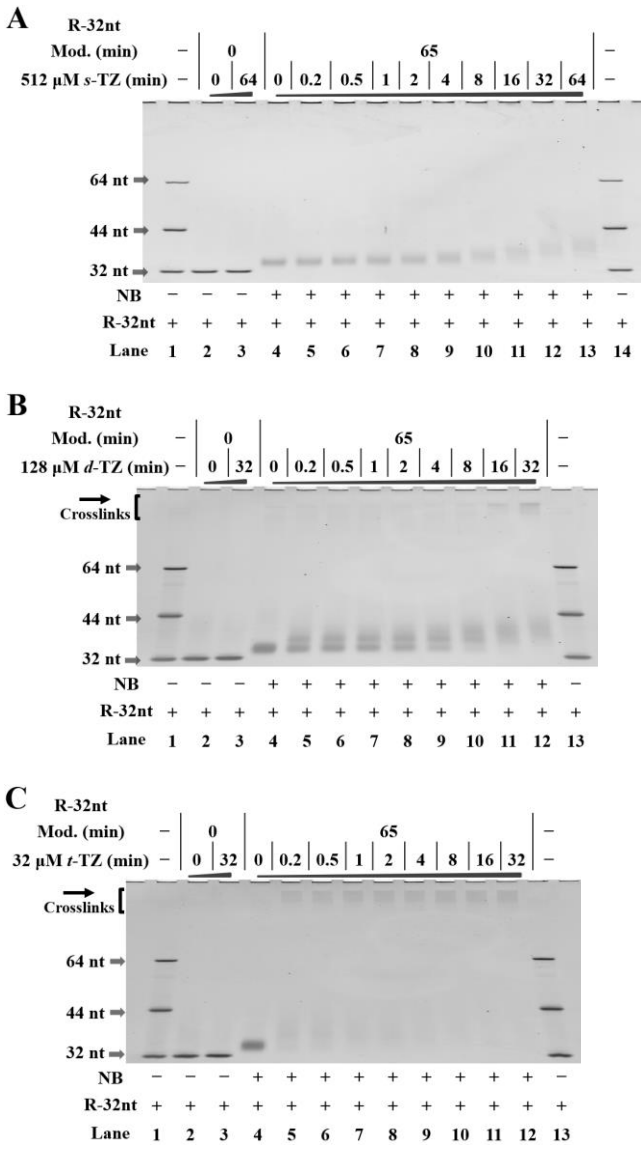

Figure S3. Time course of RNA-based NB-TZ ligation chemistry.

Reactions were performed as described in the Experimental Section. The treatment for each sample is indicated by the signs at the bottom of each lane. All samples were tested in three biological replicates. Image of representative data is shown here. (**A**) The time course experiment with *s*-TZ. Lanes 1, 14: RNA marker (R-32nt, R-44nt, R-64nt in Table S1); lanes 2-3 contain native R-32nt; lanes 4-13 contain NB-bearing R-32nt with a specified level of modification (a 65-min modification with 20 mM NBFI). (**B**) The time course experiment with *d*-TZ. Lanes 1, 13: RNA marker; lanes 2-3 contain native R-32nt; lanes 4-12 contain NB-bearing R-32nt with a specified level of modification (a 65-min modification with 20 mM NBFI). (**C**) The time course experiment with *t*-TZ. Lanes 1, 13: RNA marker; lanes 2-3 contain native R-32nt; lanes 4-12 contain NB-bearing R-32nt with a specified level of modification (a 65-min modification with 20 mM NBFI).

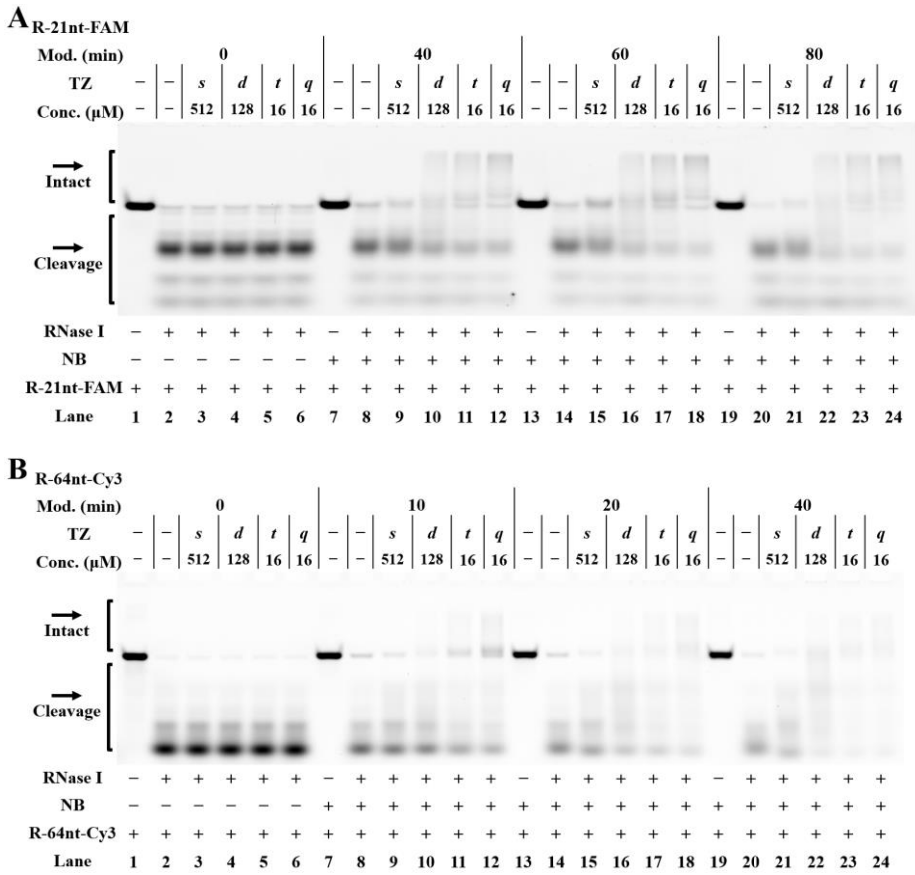

Figure S4. RNase protection assay to characterize RNA-based NB-TZ ligation chemistry.

Reactions were performed as described in the Experimental Section. The treatment for each sample is indicated by the signs at the bottom of each lane. For the TZ treatment, the letters *s*, *d*, *t* and *q* represent *s*-TZ, *d*-TZ, *t*-TZ and *q*-TZ, respectively. All samples were tested in three biological replicates. Image of representative data is shown here. (**A**) NB-TZ ligation chemistry with R-21nt-FAM. Lanes 1-6 contain native R-21nt-FAM; lanes 7-12, 13-18, 19-24 contain NB-bearing R-21nt-FAM with increasing modification levels. (**B**) NB-TZ ligation chemistry with R-64nt-Cy3. Lanes 1-6 contain native R-64nt-Cy3; lanes 7-12, 13-18, 19-24 contain NB-bearing R-64nt-Cy3 with increasing modification levels.

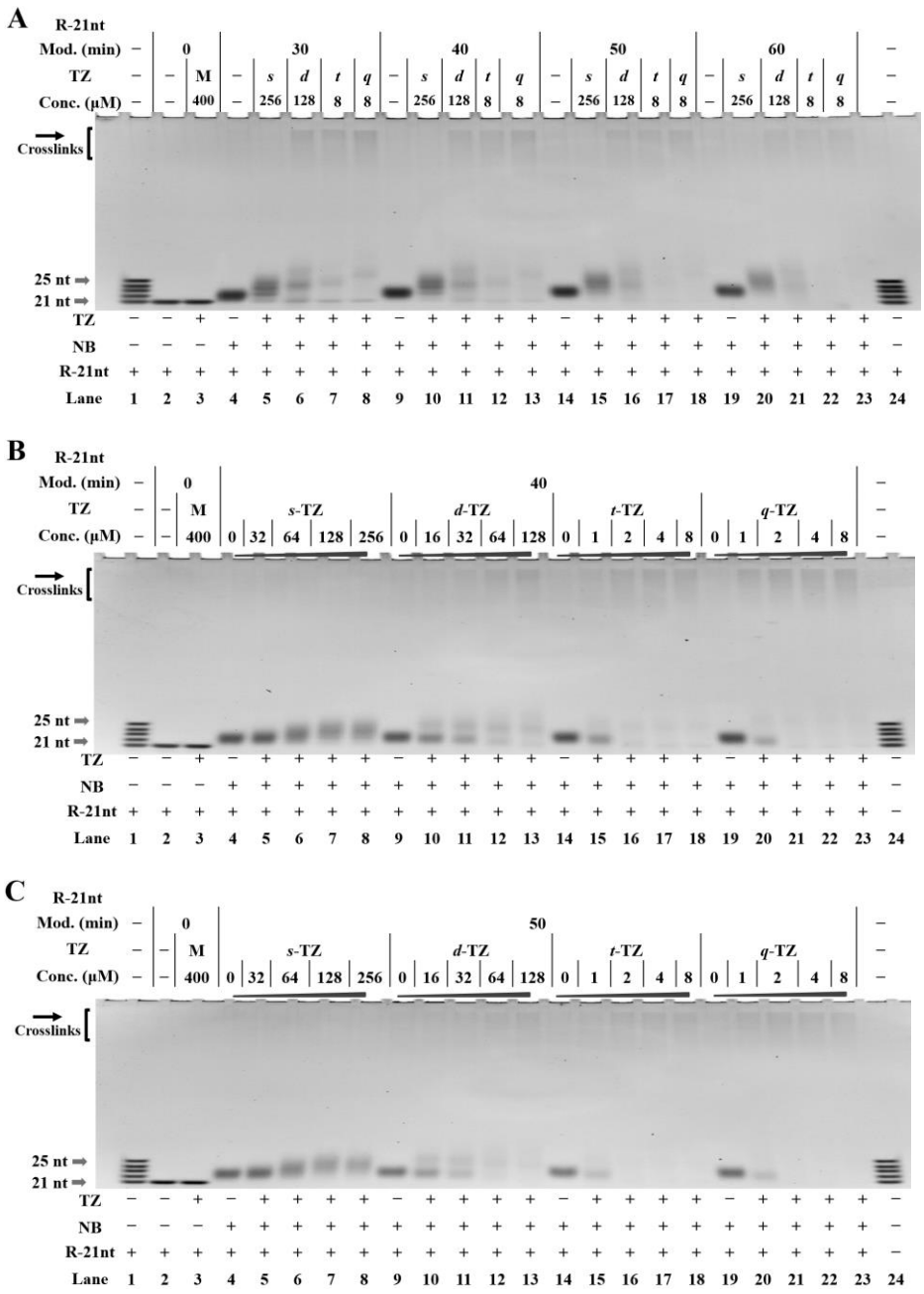

Figure S5. Gel electrophoretic characterization of RNA-based NB-TZ ligation chemistry (R-21nt). Reactions were performed as described in the Experimental Section. All samples were tested in three biological replicates. Image of representative data is shown here. For the TZ treatment, the capital letter M indicates the cotreatment with *s*-TZ (256 μM), *d*-TZ (128 μM), *t*-TZ (8 μM) and *q*-TZ (8 μM). (**A**) For the TZ treatment, the letters *s*, *d*, *t* and *q* represent *s*-TZ, *d*-TZ, *t*-TZ and *q*-TZ, respectively. Lanes 1, 24: RNA marker (R-21nt, R-22nt, R-23nt, R-24nt, R-25nt in Table S1); lanes 2-3 contain native R-21nt; lanes 4-8, 9-13, 14-18, 19-23 contain NB-bearing R-21nt with increasing modification levels. (**B**) Lanes 1, 24: RNA marker; lanes 2-3 contain native R-21nt; lanes 4-8, 9-13, 14-18, 19-23 contain NB-bearing R-21nt (a 40-min modification with 20 mM NBFI). (**C**) Lanes 1, 24: RNA marker; lanes 2-3 contain native R-21nt; lanes 4-8, 9-13, 14-18, 19-23 contain NB-bearing R-21nt (a 50-min modification with 20 mM NBFI).

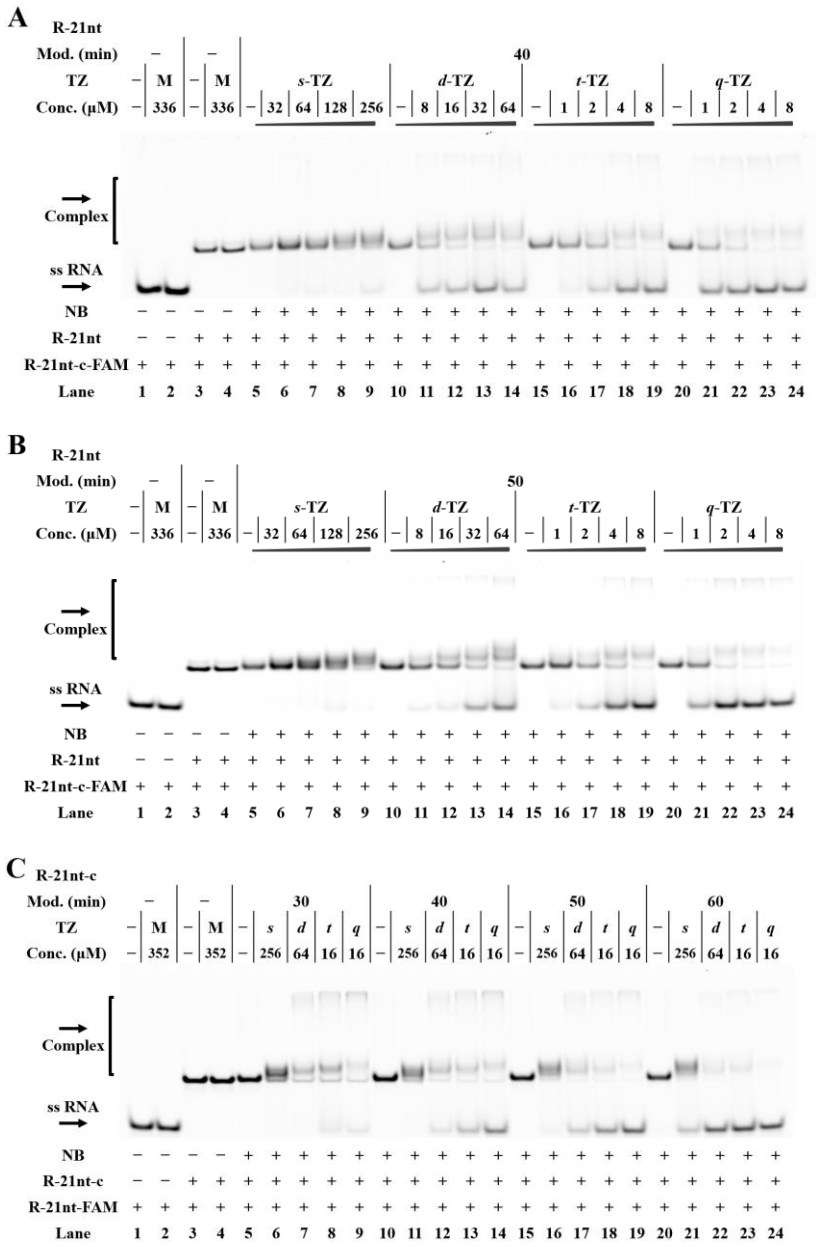

Figure S6. NB-TZ ligation chemistry for controlling RNA hybridization.

Reactions were performed as described in the Experimental Section. The treatment for each sample is indicated by the signs at the bottom of each lane. All samples were tested in three biological replicates. Image of representative data is shown here. (**A**) and (**B**) Mobility shifts of R-21nt-c-FAM upon hybridization with R-21nt with different treatments. Lanes 1-2: control without R-21nt; lanes 3-4 contain native R-21nt; lanes 5-9 (*s*-TZ), 10-14 (*d*-TZ), 15-19 (*t*-TZ), 20-24 (*q*-TZ) contain NB-bearing R-21nt. (**C**) Mobility shifts of R-21nt-FAM upon hybridization with R-21nt-c with different treatments. For the TZ treatment, the letters *s*, *d*, *t* and *q* represent *s*-TZ, *d*-TZ, *t*-TZ and *q*-TZ, respectively. The capital letter M indicates the cotreatment with *s*-TZ (256 μM), *d*-TZ (64 μM), *t*-TZ (16 μM) and *q*-TZ (16 μM). Lanes 1-2: control without R-21nt-c; lanes 3-4 contain native R-21nt-c; lanes 5-9, 10-14, 15-19, 20-24 contain NB-bearing R-21nt-c with increasing modification levels.

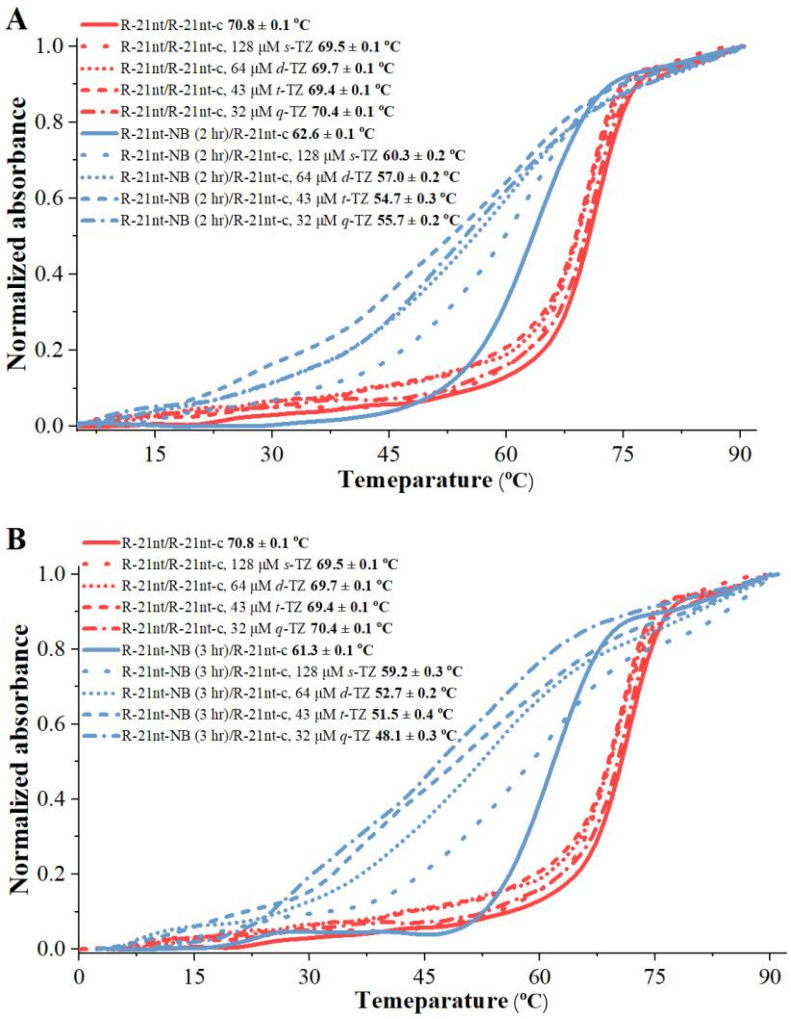

Figure S7. UV melting studies to characterize RNA-based NB-TZ ligation chemistry.

In this study, the native, NB-bearing and NB-TZ-treated RNAs were incubated with complementary strands in a 1:1 molar ratio. The absorbance of each sample at 260 nm was monitored in a Tris-HCl buffer (10 mM, pH 7.4) containing 50 mM NaCl. All normalized melting curves were temperature-overlaid for illustration purposes.

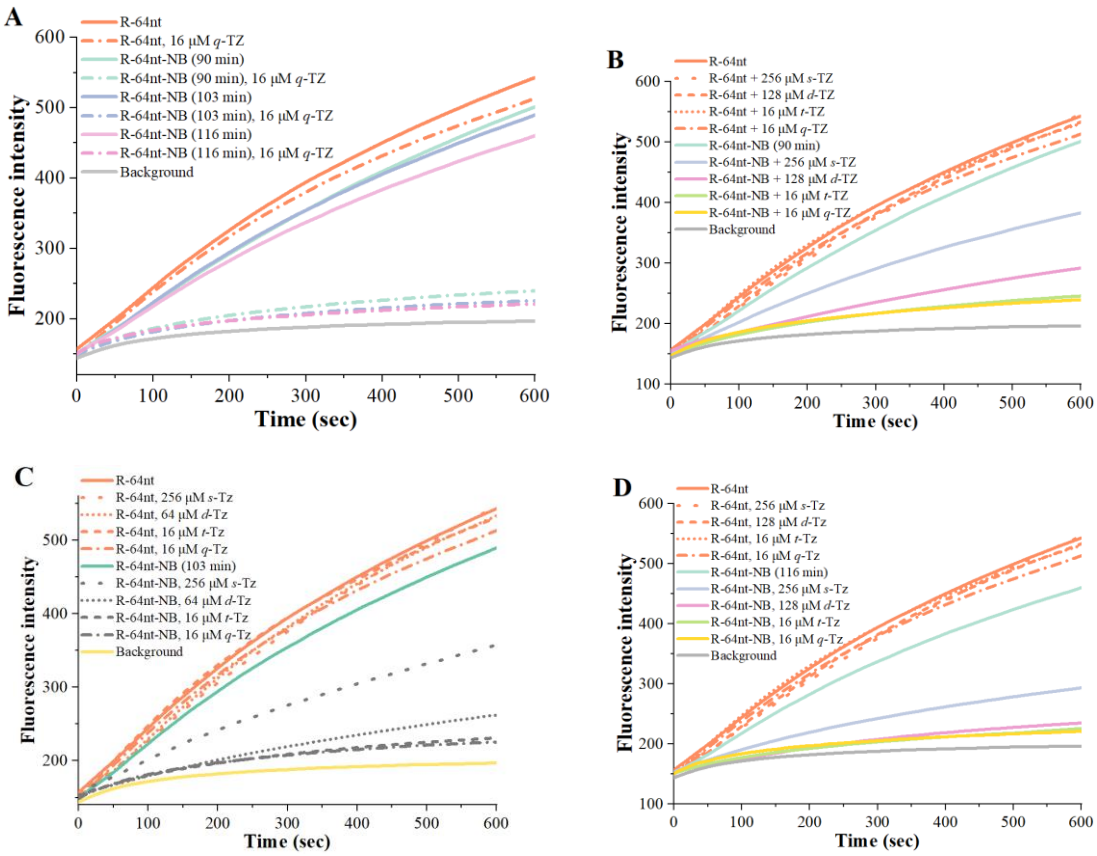

Figure S8. Molecular beacon-based assays to characterize RNA-based NB-TZ ligation chemistry.

In this study, native, NB-bearing or NB-TZ-treated RNA was mixed with molecular beacons and tested for hybridization in a fluorescence spectrofluorimeter. (**A**) In this study, NB-bearing RNAs in varying levels of modification were tested. (**B**) In this study, NB-bearing RNAs with a specified level of modification (a 90-min modification with 20 mM NBFI) were treated with different TZ derivatives. (**C**) In this study, NB-bearing RNAs with a specified level of modification (a 103-min modification with 20 mM NBFI) were treated with different TZ derivatives. (**D**) In this study, NB-bearing RNAs with a specified level of modification (a 116-min modification with 20 mM NBFI) were treated with different TZ derivatives.

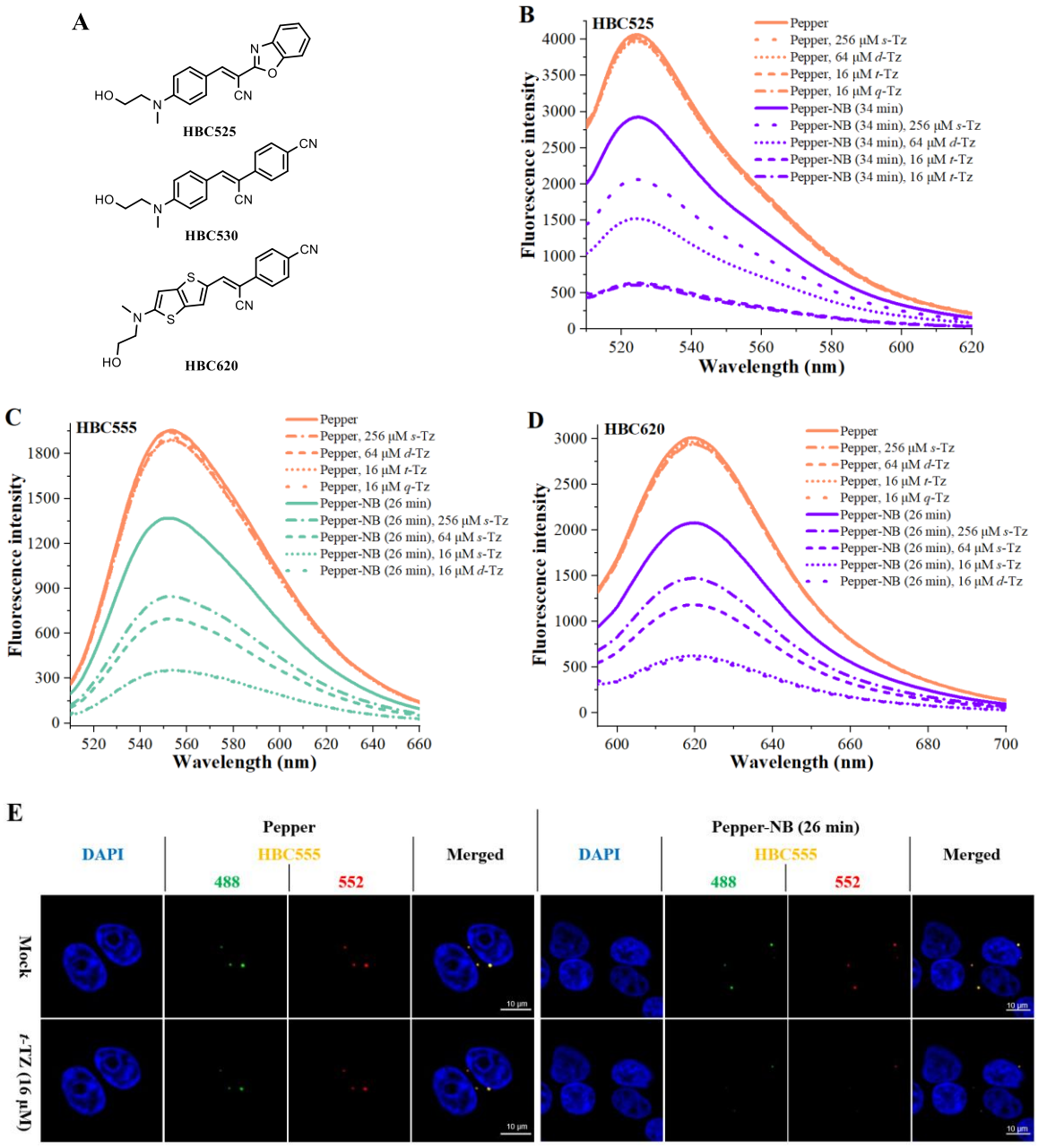

Figure S9. Demonstration of clickable RNA switches *in vitro* and in living cells.

Reactions were performed as described in the Experimental Section. All samples were tested in three biological replicates. Image of representative data was shown here. (**A**) Structures of HBC derivatives in this study. (**B**)-(**D**): Fluorescence response analysis of NB-TZ ligation chemistry on Pepper complexed with HBC525 (**B**), HBC555 (**C**), HBC620 (**D**). (**E**) Effect of NB-TZ ligation reactions on Pepper's intracellular fluorescence when stained with HBC555. HEK293T cells transfected with Pepper were labeled with 2 μM HBC555 and imaged. The nucleus was stained with Hoechst 33342 (blue). The fields of view were randomly selected for each cell slide. Scale bars: 10 μm.

A

>gi|74230048|gb|CH471062.2|:13429990-13430610 Homo sapiens 211000035832302 genomic scaffold, whole genome shotgun sequence

GCCGCTTCGAAAGTGACTGGTGCCTCGCCGCCTCCTCTCGGTGCGGGACCATGAAGCTGCTGC
CGTCGGTGGTGCTGAAGCTCTTTCTGGCTGCAGGTAAGAGGGCTGCCGACGCCCCCGGAGATC
GGGGGGATGGGGGGCGTTGTGCTGGGGGCATGGGGGAAGGTCGCCGCAGCGCACCCGGCACG
GGCCACTTGGTGGGGCCCTTGCGCTCTGGCGGACGGGCGTCGGCATCGGTGCGTGTTGGTCAG
GGGTCTGGGCGGGTGTCTGATGCGGCCTGGCCTCTCGCCCGCA**GTTCTCTCGGCACTGGT^G**
ACTGGCGAGAGCCTGGAGCGGCTTCGGAGAGGGCTAGCTGCTGGAACCAGCAACCCGGACCC
TCCCACTGTATCCACGGACCAGCTGCTACCCCTAGGAGGCGGCCGGGACCGGAAAGTCCGTG
ACTTGCAAGAGGCAGATCTGGACCTTTTGAGAGGTGGGTGTGGAGGCCCCCCATCCTTGGACC
TTGGTGGGCTGTTGAAGAATAAGCAGATCCAAGATTCTTGCTGTTTGGGCAATACTGTGGGTT
GAGGGTATTCATGGAGAACCTCGGGGAAAAGCTGATCGGCCTGATGGGCACTGGGGGATC

B

>20 dna:chromosome chromosome:GRCh38:20:10435305:10636829:1

TTATCCGGCACTGTGAAAGCTACCTTTCCTTTCTCACAATCTTTCGCACCGAATATATGTTCCA
TTCTTGAGCTAGTCATTTTCCAATGTTAAGAAAACACACCACAGAAAAGCGTTTTTTTTTCTCT
CGGTCAGTTCAACTGCCTAGCACCGTGAGTTACCATGATACGTTATTTGCTAATGAGAGTCAT
TGGGGTCCCAGCCTTTAAAAATAGCCTGCGTCCGGCGCCATTTTTGTTTTGGGCCCACTTTGAA
AGCCGCGATATTCTGAACAGAGGCCATTTTTCTTTTGGGCAGATTCCACGGGCCATCGAAGTG
TTTCGCTGCCA**TCT^TAAATCCTGGCTGTGGC**CTCAATCCTGCAGCGAAGCTGCCCAGATCA
TTTTGTGTTTGGGCGGCGGCTGAGTTCCCAAACGCGCGCGGAGACCCTGGGAAGGAGGAAGT
AAGCGCGAAAGTGCTTCCCTTAAGCTTCTGAAGGTTGGCTGCAGTTCCGGCTACCTGTGTAGT
CCGAGTTTCCACAGCCAGGTACTACTCCGCCAGTGACCCTGGACAGTAACAAAACATATAAA
GCCCGAGCCCAAACCCCGCCACCATCATAGGTAAGCACATGGACCTCTGACAACCTCAGATGT
TCCTTCAAGTGAACTGAACTGTTTGCCCATCTCCTCCCTCCTGGTTTTTGGCTTTGATTTTTTGA
GACTTTTCCGAATCCTTCTCCCTGTACTTCCACCTTTCTTCATTGTTTTCAAAAAGCCAAAAAG
TTGCTAAACATCAGG

C

>X dna:chromosome chromosome:GRCh38:X:134460165:134520513:1

GTTGTGATAAAAGGTGATGCTCACCTCTCCCACACCCTTTTATAGTTTAGGGATTGTATTTCCA
AGGTTTCTAGACTGAGAGCCCTTTTCATCTTTGCTCATTGACACTCTGTACCCATTAATCCTCC
TTATTAGCTCCCCTTCAATGGACACATGGGTAGTCAGGGTGCAGGTCTCAGAACTGTCCTTCA
GGTTCCAGGTGATCAACCAAGTGCCTTGTCTGTAGTGTCAACTCATTGCTGCCCCTTCCTAGTA
ATCCCCATAATTTAGCTCTCCA**TTT^CATAGTCTTTCCTTGGG**TGTGTTAAAAGTGACCATGG
TACACTCAGCACGGATGAAATGAAACAGTGTTTAGAAACGTCAGTCTTCTCTTTTGTAATGCC
CTGTAGTCTCTCTGTATGTTATATGTCACATTTTGTAATTAACAGCTTGCTGGTGAAAAGGACC
CCACGAAGTGTTGGATATAAGCCAGACTGTAAGTGAATTACTTTTTTTGTCAATCATTTAACCA
TCTTTAACCTAAAAGAGTTTTATGTGAAATGGCTTATAATTGCTTAGAGAATATTTGTAGAGA
GGCACATTTGCCAGTATTAGATTTAAAAGTGATGTTTTCTTTATCTAAATGATGAATTATGATT
CTTTTTAGTTGTTGGATTTGAAATTCCAGACAAGTTTGTTGTAGGATATGCCCTTGACTATAAT
GAATACTTCAGGGATTTGAATGTAAGTAATTGCTTCTTTTTCTCACTCATTTTTCAAAACACGC
ATAAAAATTTAGGAAAGAGAATTGTTTTCTCCTTCCAGCACCTCATAATTTGAACAGACTGAT
GGTTCCCATTAGTCACATAAAGCTGTAGTCTAGTACAGACGTCCTTAGAACTGGAACCTGGCC
AGGCTAGGGTGACACTTCTTGTTGGCTGAAATAGTTGAACAGCTTTAATATACAATAATTGTT
GCATTATTATTTCAGATGATAAATGTGGTCATAAGTAAGAAATAAATGATCGAGTTTAGTCTT
TTAATTCACTGTCCTTTGAATACCTGCCTCTTACTCTGGAGGCAGAAGTCCCATGGATGTGTTT
ATGA

Figure S10. Location of sequences recognised by gRNAs and PCR primers.

The target loci and PCR primer loci were indicated by blue color and underlining, respectively. Red caret showed the cleavage sites by Cas9 nuclease. PCR primers flanking the target regions were designed by BLAST search and procedures. (**A**) Schematic illustration of the 5'-UTR sequence of *HBEGF* gene around target loci. We generated target HBEGF DNA (t-HBEGF) carrying the target loci from HeLa-OC genomic

DNA. The 20-nt sequence was the exact same sequence as the target sequence. (**B**) Schematic illustration of the sequence of *SLX4IP* gene around target loci. The SLX4IP gene is located on the short arm (p) of chromosome 20 at position 12.2 (20p12.2). We generated target SLX4IP DNA (t-SLX4IP) carrying the target loci from HeLa-OC genomic DNA. The 20-nt sequence was the exact same sequence as the target sequence. (**C**) Schematic illustration of the sequence of *HPRT1* gene around target loci. We generated target HPRT1 DNA (t-HPRT1) carrying the target loci from HeLa-OC genomic DNA. The 20-nt sequence was the exact same sequence as the target sequence.

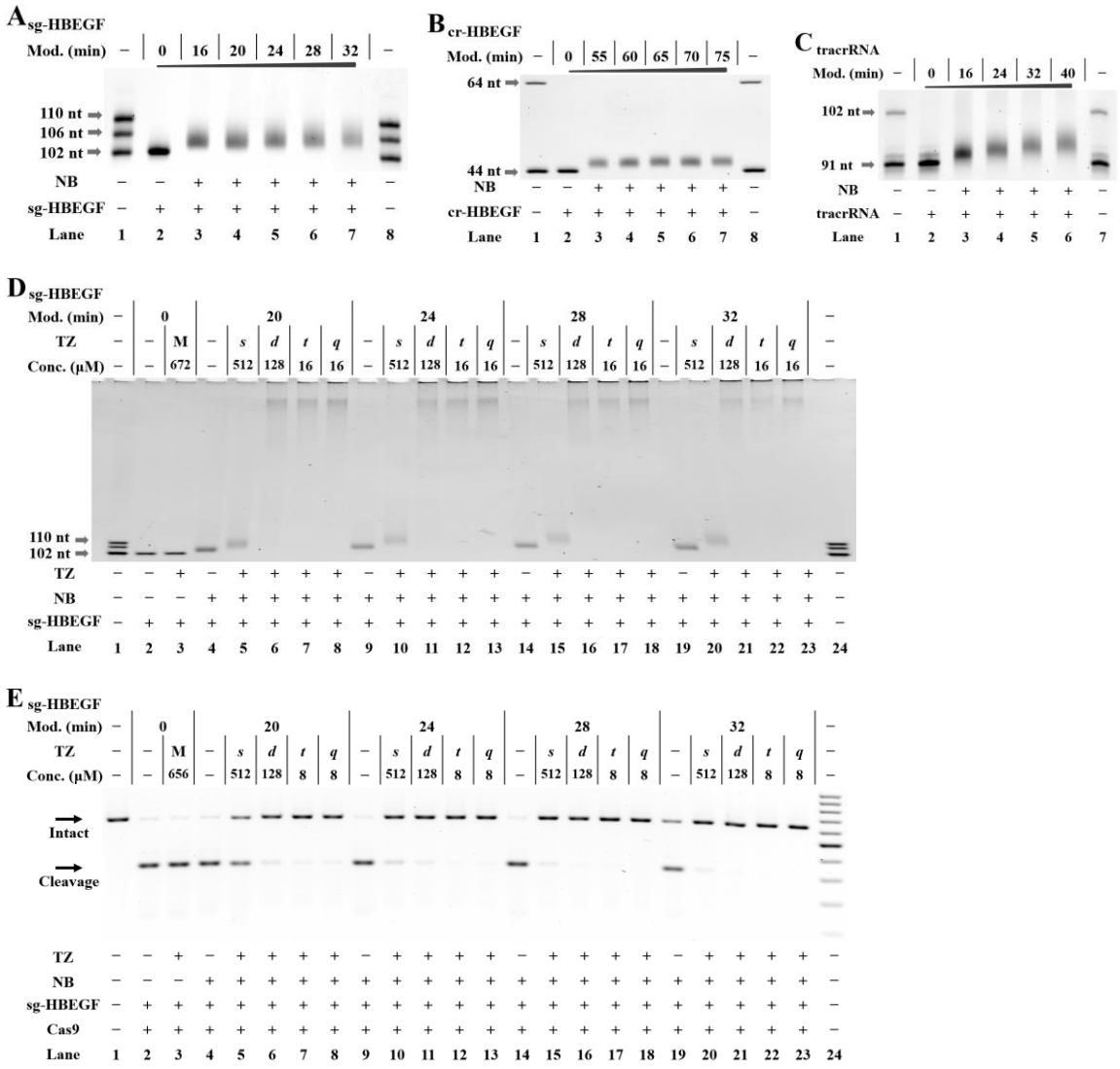

Figure S11. RNA-based NB-TZ ligation chemistry for controlling CRISPR/Cas9.

Reactions were performed as described in the Experimental Section. All samples were tested in three biological replicates. Image of representative data was shown here. (**A**) The extents of modification of sg-HBEGF. Lanes 1, 8: RNA size-marker (R-102nt, R-106nt, R-110nt); lane 2 contains native sg-HBEGF; lanes 3-7 contain NB-bearing sg-HBEGF with increasing modification levels. (**B**) The extents of modification of cr-HBEGF. Lanes 1, 8: RNA size-marker (R-44nt, R-64nt); lane 2 contains native cr-HBEGF; lanes 3-7 contain NB-bearing cr-HBEGF with increasing modification levels. (**C**) The extents of modification of tracrRNA. Lanes 1, 7: RNA size-marker (tracrRNA, R-102nt); lane 2 contains native tracrRNA; lanes 3-6 contain NB-bearing tracrRNA with increasing modification levels. (**D**) NB-TZ ligation chemistry with sg-HBEGF. The capital letter M indicates the cotreatment with *s*-TZ (256 μM), *d*-TZ (128 μM), *t*-TZ (16 μM) and *q*-TZ (16 μM). Lanes 1, 24: RNA marker (R-102nt, R-106nt, R-110nt); lanes 2-3 contain native sg-HBEGF; lanes 4-8, 9-13, 14-18, 19-23 contain NB-bearing sg-HBEGF with increasing modification levels. (**E**) Modification-dependent inhibition of CRISPR/Cas9 with NB-TZ ligation chemistry. The capital letter M indicates the cotreatment with *s*-TZ (512 μM), *d*-TZ (128 μM), *t*-TZ (8 μM) and *q*-TZ (8 μM). Lane 1: no Cas9 control; lanes 2-3 contain native sg-HBEGF; lanes 4-8, 9-13, 14-18, 19-23 contain NB-bearing sg-HBEGF with increasing modification levels; lane 24: DNA marker (GeneRuler 100-bp DNA Ladder). For (**D**) and (**E**), the letters *s*, *d*, *t* and *q* represent *s*-TZ, *d*-TZ, *t*-TZ and *q*-TZ, respectively.

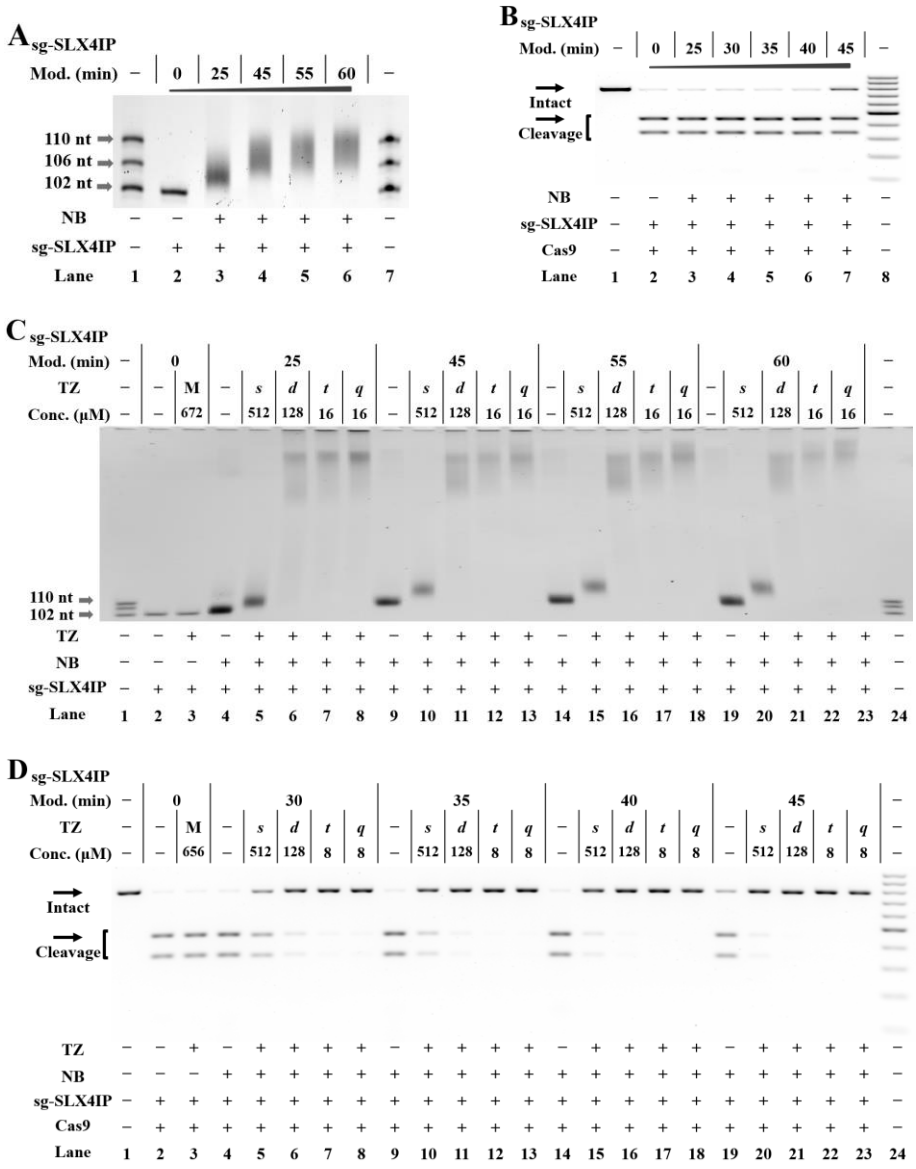

Figure S12. RNA-based NB-TZ ligation chemistry for controlling CRISPR/Cas9 with sg-SLX4IP.

Reactions were performed as described in the Experimental Section. All samples were tested in three biological replicates. Image of representative data was shown here. (**A**) The extents of modification of sg-SLX4IP. Lanes 1, 7: RNA size-marker (R-102nt, R-106nt, R-110nt); lane 2 contains native sg-SLX4IP; lanes 3-6 contain NB-bearing sg-SLX4IP with increasing modification levels. (**B**) Tolerance of CRISPR/Cas9 to NB-bearing sg-SLX4IP. Lane 1: no Cas9 control; lane 2 contains native sg-SLX4IP; lanes 3-7 contain NB-bearing sg-SLX4IP with increasing modification levels; lane 8: DNA marker (GeneRuler 100-bp DNA Ladder). (**C**) NB-TZ ligation chemistry with sg-SLX4IP. The capital letter M indicates the cotreatment with *s*-TZ (512 μM), *d*-TZ (128 μM), *t*-TZ (16 μM) and *q*-TZ (16 μM). Lanes 1, 24: RNA marker (R-102nt, R-106nt, R-110nt); lanes 2-3 contain native sg-SLX4IP; lanes 4-8, 9-13, 14-18, 19-23 contain NB-bearing sg-SLX4IP with increasing modification levels. (**D**) Modification-dependent inhibition of CRISPR/Cas9 with sg-SLX4IP. The capital letter M indicates the cotreatment with *s*-TZ (512 μM), *d*-TZ (128 μM), *t*-TZ (8 μM) and *q*-TZ (8 μM). Lane 1: no Cas9 control; lanes 2-3 contain native sg-SLX4IP; lanes 4-8, 9-13, 14-18, 19-23 contain NB-bearing sg-SLX4IP with increasing modification levels; lane 24: DNA marker. For (**C**) and (**D**), the letters *s*, *d*, *t* and *q* represent *s*-TZ, *d*-TZ, *t*-TZ and *q*-TZ, respectively.

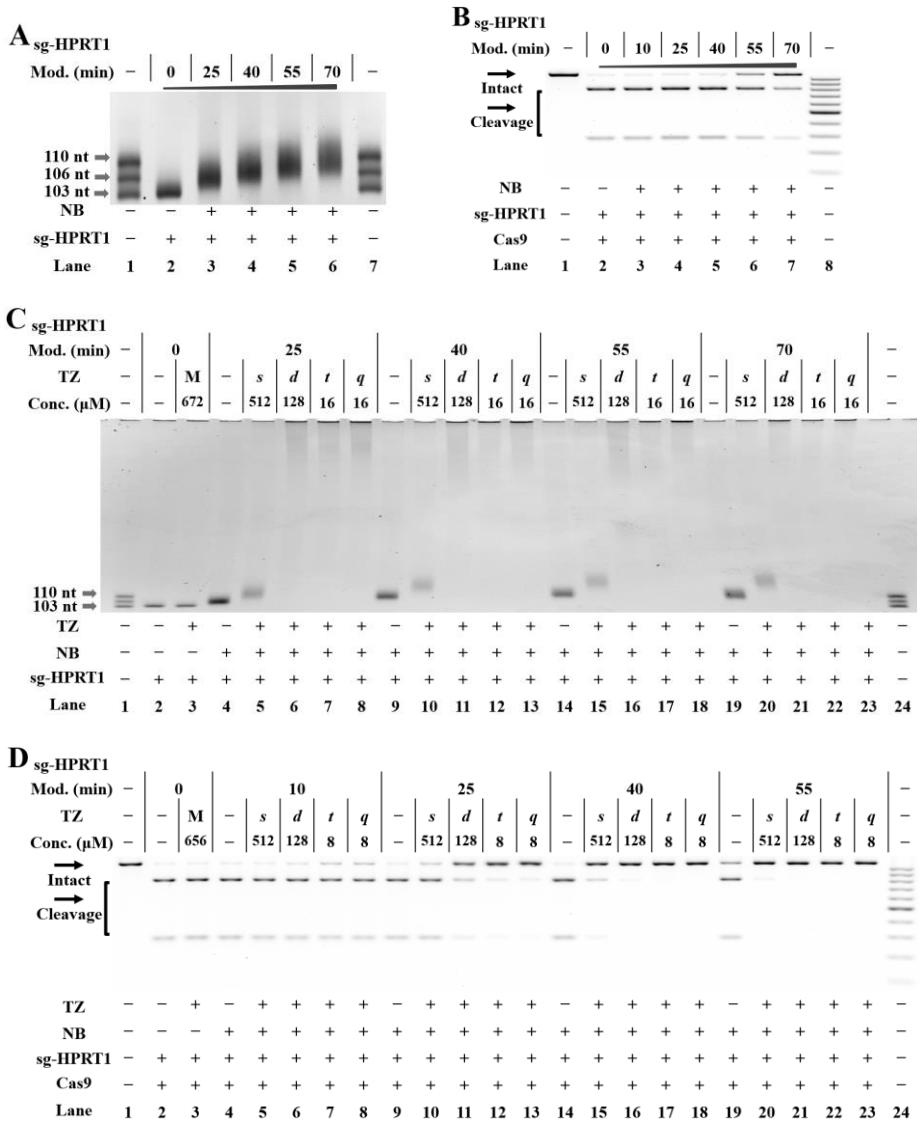

Figure S13. RNA-based NB-TZ ligation chemistry for controlling CRISPR/Cas9 with sg-HPRT1.

Reactions were performed as described in the Experimental Section. All samples were tested in three biological replicates. Image of representative data was shown here. (**A**) The extents of modification of sg-sg-HPRT1. Lanes 1, 7: RNA size-marker (sg-HPRT1, R-106nt, R-110nt); lane 2 contains native sg-HPRT1; lanes 3-6 contain NB-bearing sg-HPRT1 with increasing modification levels. (**B**) Tolerance of CRISPR/Cas9 to NB-bearing sg-HPRT1. Lane 1: no Cas9 control; lane 2 contains native sg-HPRT1; lanes 3-7 contain NB-bearing sg-HPRT1 with increasing modification levels; lane 8: DNA marker (GeneRuler 100-bp DNA Ladder). (**C**) NB-TZ ligation chemistry with sg-HPRT1. The capital letter M indicates the cotreatment with *s*-TZ (512 μM), *d*-TZ (128 μM), *t*-TZ (16 μM) and *q*-TZ (16 μM). Lanes 1, 24: RNA marker (sg-HPRT1, R-106nt, R-110nt); lanes 2-3 contain native sg-HPRT1; lanes 4-8, 9-13, 14-18, 19-23 contain NB-bearing sg-HPRT1 with increasing modification levels. (**D**) Modification-dependent inhibition of CRISPR/Cas9 with sg-HPRT1. The capital letter M indicates the cotreatment with *s*-TZ (512 μM), *d*-TZ (128 μM), *t*-TZ (8 μM) and *q*-TZ (8 μM). Lane 1: no Cas9 control; lanes 2-3 contain native sg-HPRT1; lanes 4-8, 9-13, 14-18, 19-23 contain NB-bearing sg-HPRT1 with increasing modification levels; lane 24: DNA marker. For (**C**) and (**D**), the letters *s*, *d*, *t* and *q* represent *s*-TZ, *d*-TZ, *t*-TZ and *q*-TZ, respectively.

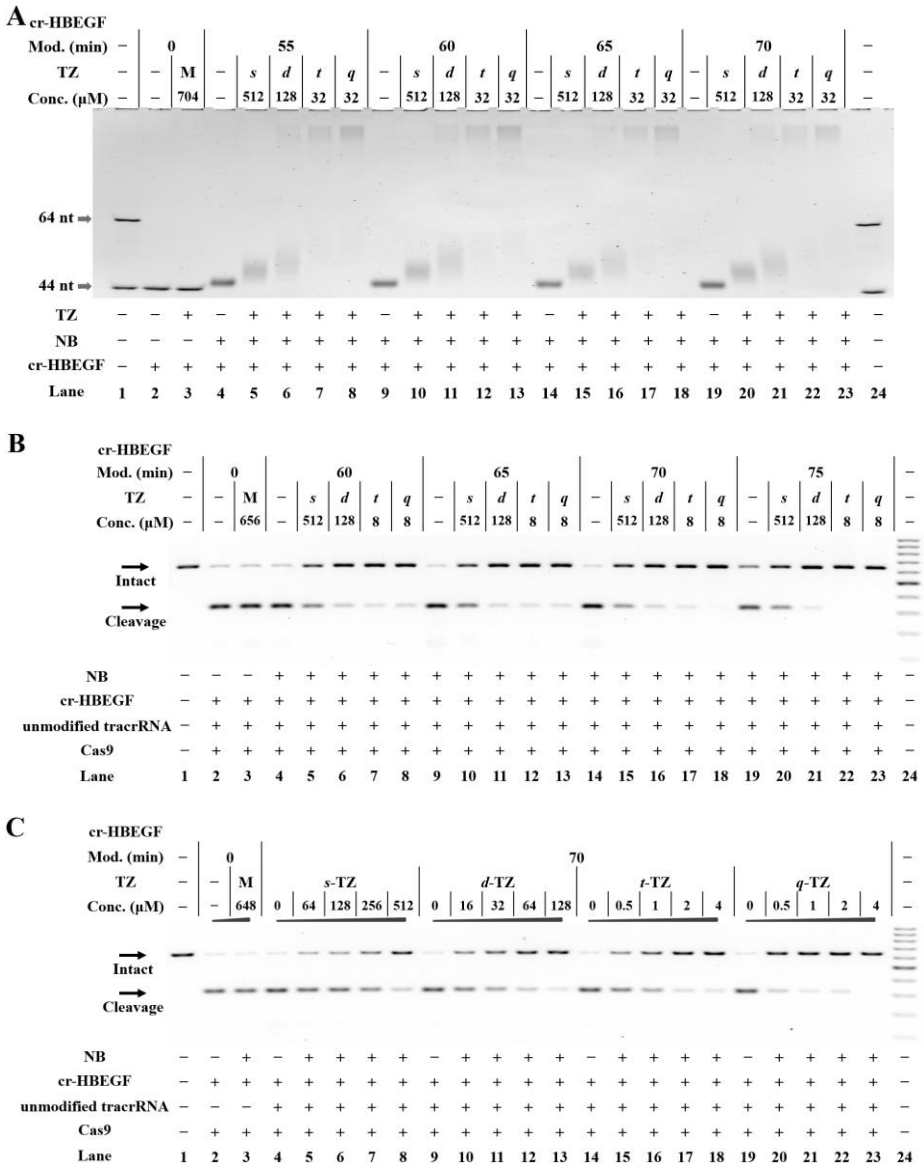

Figure S14. RNA-based NB-TZ ligation chemistry for controlling CRISPR/Cas9 with cr-HBEGF and native tracrRNA.

Reactions were performed as described in the Experimental Section. The treatment for each sample is indicated by the signs at the bottom of each lane. For the TZ treatment, the letters *s*, *d*, *t* and *q* represent *s*-TZ, *d*-TZ, *t*-TZ and *q*-TZ, respectively. (**A**) NB-TZ ligation chemistry with cr-HBEGF. The capital letter M indicates the cotreatment with *s*-TZ (512 μM), *d*-TZ (128 μM), *t*-TZ (32 μM) and *q*-TZ (32 μM). Lanes 1, 24: RNA marker (R-44nt, R-64nt); lanes 2-3 contain native cr-HBEGF; lanes 4-8, 9-13, 14-18, 19-23 contain NB-bearing cr-HBEGF with increasing modification levels. (**B**) Modification-dependent inhibition of CRISPR/Cas9 with NB-bearing cr-HBEGF. The capital letter M indicates the cotreatment with *s*-TZ (512 μM), *d*-TZ (128 μM), *t*-TZ (8 μM) and *q*-TZ (8 μM). Lane 1: no Cas9 control; lanes 2-3 contain native cr-HBEGF; lanes 4-8, 9-13, 14-18, 19-23 contain NB-bearing cr-HBEGF with increasing modification levels; lane 24: DNA marker (GeneRuler 100-bp DNA Ladder). (**C**) Dose-dependent effect of TZ on inhibition of CRISPR/Cas9 with NB-bearing cr-HBEGF. The capital letter M indicates the cotreatment with *s*-TZ (512 μM), *d*-TZ (128 μM), *t*-TZ (4 μM) and *q*-TZ (4 μM). Lane 1: no Cas9 control; lanes 2-3 contain native cr-HBEGF; lanes 4-8, 9-13, 14-18, 19-23 contain NB-bearing cr-HBEGF (a 70-min modification with 20 mM NBFI); lane 24: DNA marker.

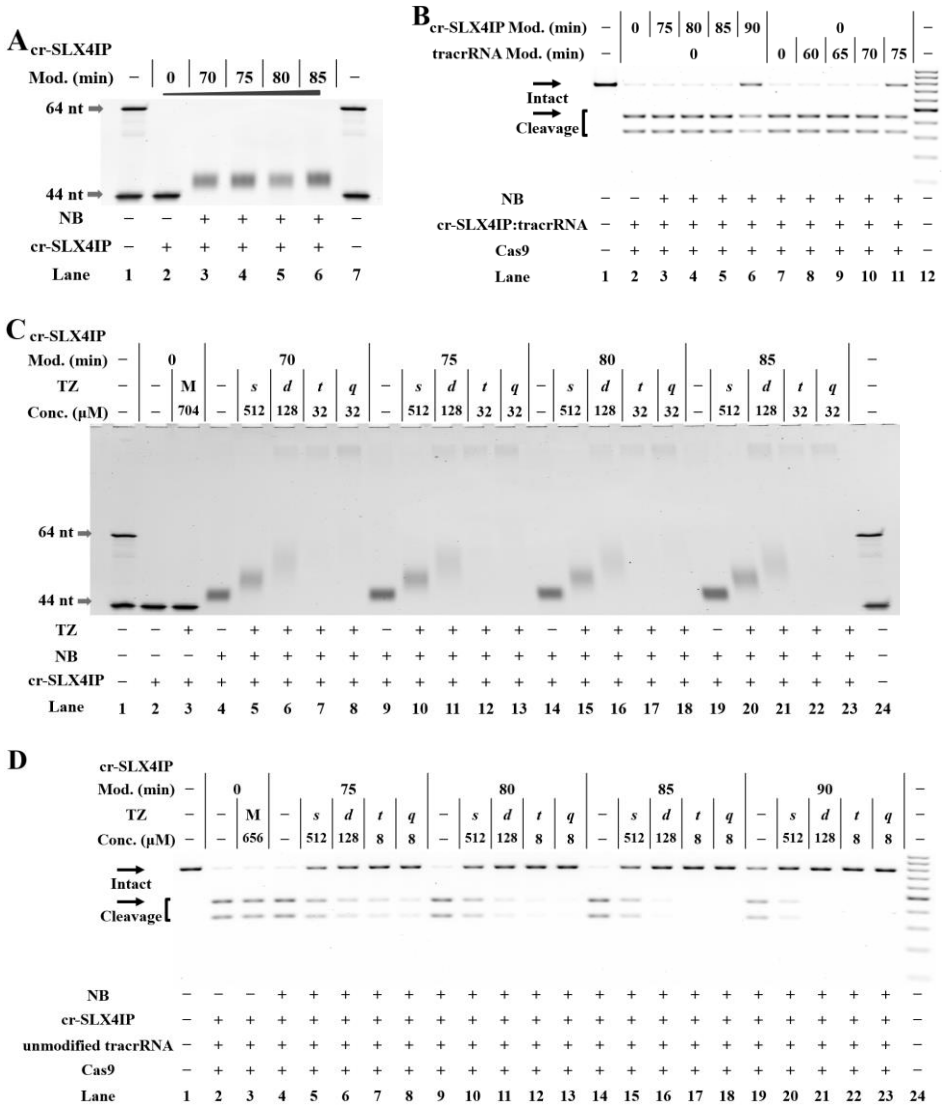

Figure S15. RNA-based NB-TZ ligation chemistry for controlling CRISPR/Cas9 with cr-SLX4IP and native tracrRNA.

Reactions were performed as described in the Experimental Section. The treatment for each sample is indicated by the signs at the bottom of each lane. For the TZ treatment, the letters *s*, *d*, *t* and *q* represent *s*-TZ, *d*-TZ, *t*-TZ and *q*-TZ, respectively. (**A**) The extents of modification of cr-SLX4IP. Lanes 1, 7: RNA size-marker (R-44nt, R-64nt); lane 2 contains native cr-SLX4IP; lanes 3-6 contain NB-bearing cr-SLX4IP with increasing modification levels. (**B**) The tolerance of CRISPR/Cas9 to NB-bearing cr-SLX4IP or tracrRNA. Lane 1: no Cas9 control; lanes 2, 7 contain native cr-SLX4IP and native tracrRNA; lanes 3-6 contain native tracrRNA and NB-bearing cr-SLX4IP with increasing modification levels; lanes 8-11 contain native cr-SLX4IP and NB-bearing tracrRNA with increasing modification levels; lane 12: DNA marker (GeneRuler 100-bp DNA Ladder). (**C**) NB-TZ ligation chemistry with cr-SLX4IP. The capital letter M indicates the cotreatment with *s*-TZ (512 μM), *d*-TZ (128 μM), *t*-TZ (32 μM) and *q*-TZ (32 μM). Lanes 1, 24: RNA marker (R-44nt, R-64nt); lanes 2-3 contain native cr-SLX4IP; lanes 4-8, 9-13, 14-18, 19-23 contain NB-bearing cr-SLX4IP with increasing modification levels. (**D**) Dose-dependent effect of TZ on inhibition of CRISPR/Cas9 with NB-bearing cr-SLX4IP. The capital letter M indicates the cotreatment with *s*-TZ (512 μM), *d*-TZ (128 μM), *t*-TZ (8 μM) and *q*-TZ (8 μM). Lane 1: no Cas9 control; lanes 2-3 contain native cr-SLX4IP; lanes 4-8, 9-13, 14-18, 19-23 contain NB-bearing cr-SLX4IP with increasing modification levels; lane 24: DNA marker.

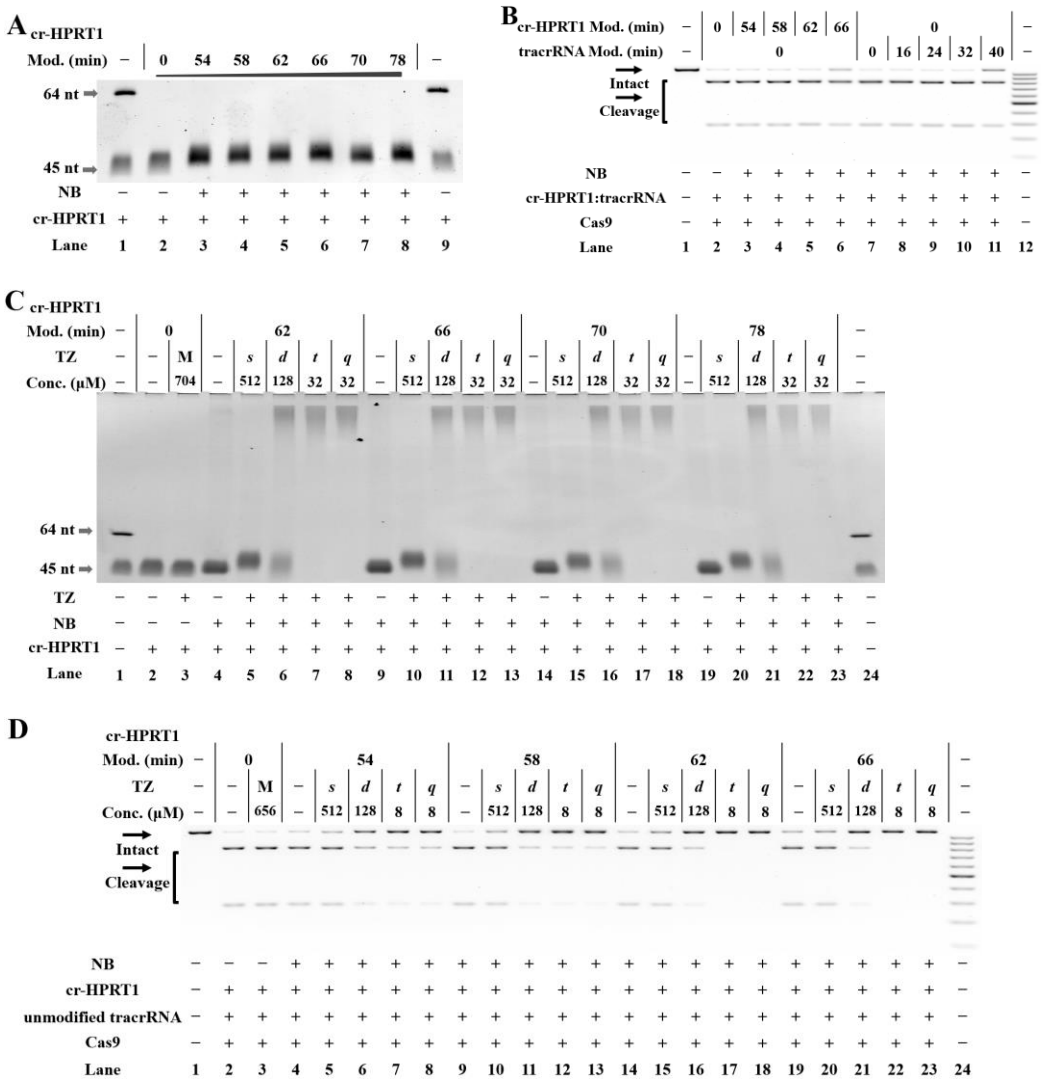

Figure S16. RNA-based NB-TZ ligation chemistry for controlling CRISPR/Cas9 with cr-HPRT1 and native tracrRNA.

Reactions were performed as described in the Experimental Section. The treatment for each sample is indicated by the signs at the bottom of each lane. For the TZ treatment, the letters *s*, *d*, *t* and *q* represent *s*-TZ, *d*-TZ, *t*-TZ and *q*-TZ, respectively. (**A**) The extents of modification of cr-HPRT1. Lanes 1, 9: RNA size-marker (cr-HPRT1, R-64nt); lane 2 contains native cr-HPRT1; lanes 3-8 contain NB-bearing cr-HPRT1 with increasing modification levels. (**B**) The tolerance of CRISPR/Cas9 to NB-bearing cr-HPRT1 or tracrRNA. Lane 1: no Cas9 control; lanes 2, 7 contain native cr-HPRT1 and native tracrRNA; lanes 3-6 contain native tracrRNA and NB-bearing cr-HPRT1 with increasing modification levels; lanes 8-11 contain native cr-HPRT1 and NB-bearing tracrRNA with increasing modification levels; lane 12: DNA marker (GeneRuler 100-bp DNA Ladder). (**C**) NB-TZ ligation chemistry with cr-HPRT1. The capital letter M indicates the cotreatment with *s*-TZ (512 μM), *d*-TZ (128 μM), *t*-TZ (32 μM) and *q*-TZ (32 μM). Lanes 1, 24: RNA marker (cr-HPRT1, R-64nt); lanes 2-3 contain native cr-HPRT1; lanes 4-8, 9-13, 14-18, 19-23 contain NB-bearing cr-HPRT1 with increasing modification levels. (**D**) Dose-dependent effect of TZ on inhibition of CRISPR/Cas9 with NB-bearing cr-HPRT1. The capital letter M indicates the cotreatment with *s*-TZ (512 μM), *d*-TZ (128 μM), *t*-TZ (8 μM) and *q*-TZ (8 μM). Lane 1: no Cas9 control; lanes 2-3 contain native cr-HPRT1; lanes 4-8, 9-13, 14-18, 19-23 contain NB-bearing cr-HPRT1 with increasing modification levels; lane 24: DNA marker.

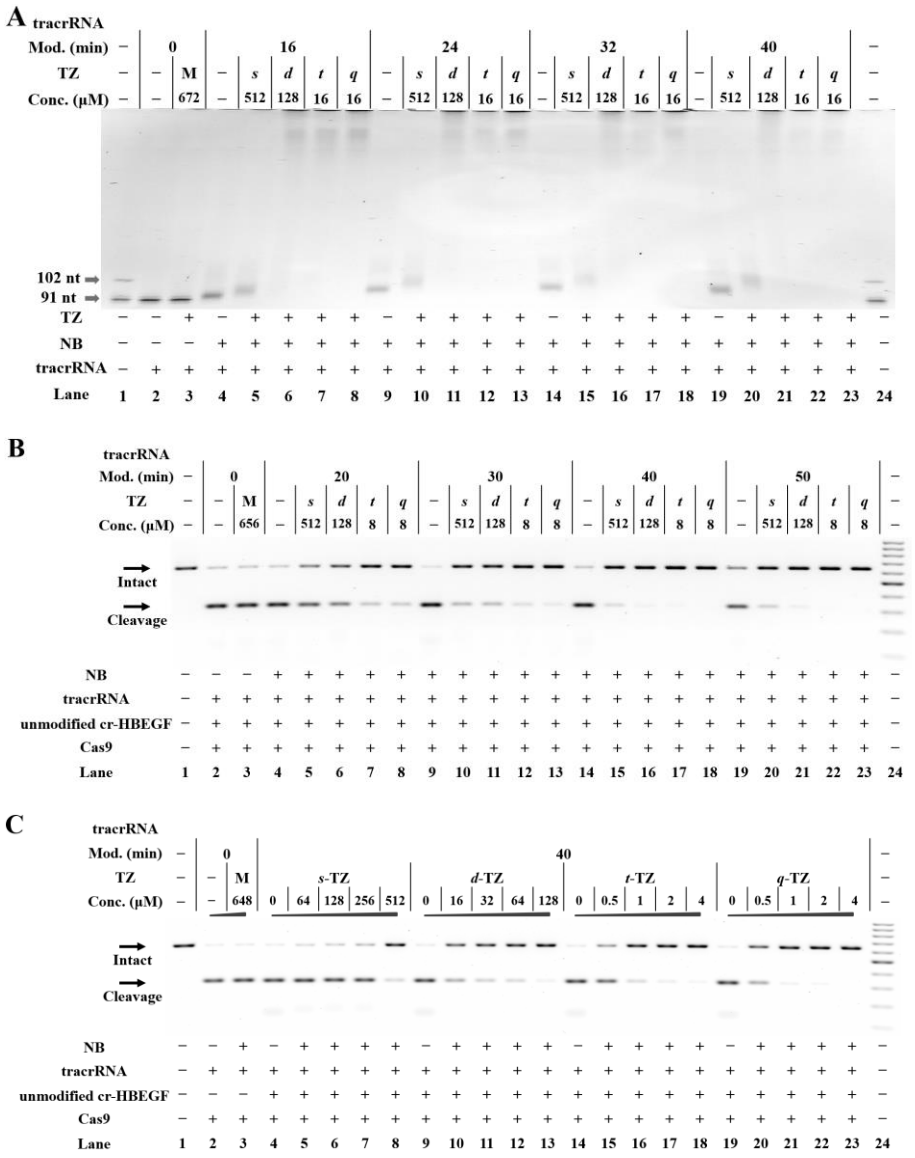

Figure S17. RNA-based NB-TZ ligation chemistry for controlling CRISPR/Cas9 with tracrRNA and cr-HBEGF.

Reactions were performed as described in the Experimental Section. For the TZ treatment, the letters *s*, *d*, *t* and *q* represent *s*-TZ, *d*-TZ, *t*-TZ and *q*-TZ, respectively. (**A**) NB-TZ ligation chemistry with tracrRNA. The capital letter M indicates the cotreatment with *s*-TZ (512 μM), *d*-TZ (128 μM), *t*-TZ (16 μM) and *q*-TZ (16 μM). Lanes 1, 24: RNA marker (tracrRNA, R-102nt); lanes 2-3 contain native tracrRNA; lanes 4-8, 9-13, 14-18, 19-23 contain NB-bearing tracrRNA with increasing modification levels. (**B**) Modification-dependent inhibition of CRISPR/Cas9 with NB-bearing tracrRNA and native cr-HBEGF. The capital letter M indicates the cotreatment with *s*-TZ (512 μM), *d*-TZ (128 μM), *t*-TZ (8 μM) and *q*-TZ (8 μM). Lane 1: no Cas9 control; lanes 2-3 contain native tracrRNA and native cr-HBEGF; lanes 4-8, 9-13, 14-18, 19-23 contain native cr-HBEGF and NB-bearing tracrRNA with increasing modification levels; lane 24: DNA marker (GeneRuler 100-bp DNA Ladder). (**C**) Dose-dependent effect of TZ on inhibition of CRISPR/Cas9 with NB-bearing tracrRNA and native cr-HBEGF. The capital letter M indicates the cotreatment with *s*-TZ (512 μM), *d*-TZ (128 μM), *t*-TZ (4 μM) and *q*-TZ (4 μM). Lane 1: no Cas9 control; lanes 2-3 contain native tracrRNA and native cr-HBEGF; lanes 4-8 (*s*-TZ), 9-13 (*d*-TZ), 14-18 (*t*-TZ), 19-23 (*q*-TZ) contain native cr-HBEGF and NB-bearing tracrRNA (a 40-min modification with 20 mM NBFI); lane 24: DNA marker.

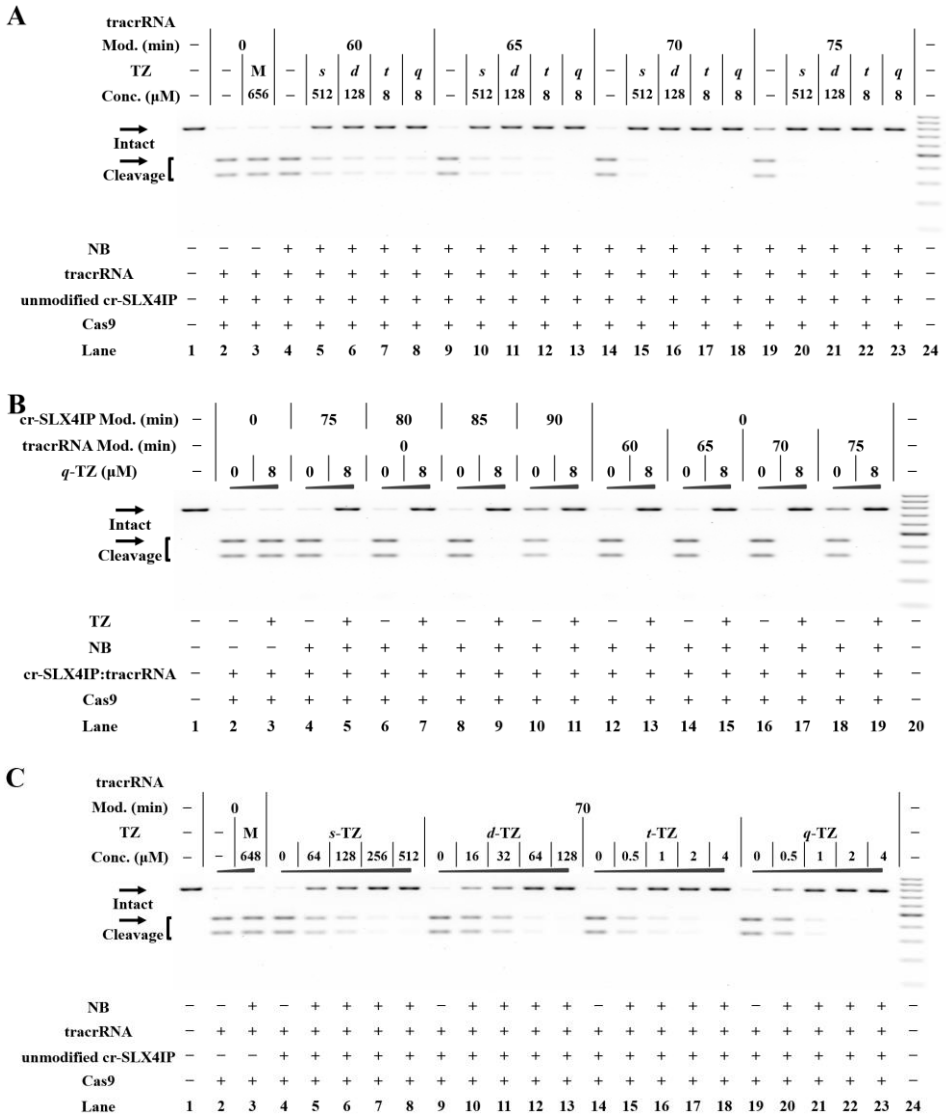

Figure S18. RNA-based NB-TZ ligation chemistry for controlling CRISPR/Cas9 with tracrRNA and cr-SLX4IP.

Reactions were performed as described in the Experimental Section. For the TZ treatment, the letters *s*, *d*, *t* and *q* represent *s*-TZ, *d*-TZ, *t*-TZ and *q*-TZ, respectively. (**A**) Modification-dependent inhibition of CRISPR/Cas9 with NB-bearing tracrRNA and native cr-SLX4IP. The capital letter M indicates the cotreatment with *s*-TZ (512 μM), *d*-TZ (128 μM), *t*-TZ (8 μM) and *q*-TZ (8 μM). Lane 1: no Cas9 control; lanes 2-3 contain native tracrRNA and native cr-SLX4IP; lanes 4-8, 9-13, 14-18, 19-23 contain native cr-SLX4IP and NB-bearing tracrRNA with increasing modification levels; lane 24: DNA marker (GeneRuler 100-bp DNA Ladder). (**B**) Modification-dependent inhibition of CRISPR/Cas9 with *q*-TZ. In this study, either cr-SLX4IP or tracrRNA was modified with the NB moieties. Lane 1: target control; lanes 2-3 contain native cr-SLX4IP and native tracrRNA; lanes 4-5, 6-7, 8-9, 10-11 contain native tracrRNA and NB-bearing cr-SLX4IP with increasing modification levels; lanes 12-13, 14-15, 16-17, 18-19 contain native cr-SLX4IP and NB-bearing tracrRNA with increasing modification levels; lane 20: DNA marker. (**C**) Dose-dependent effect of TZ on inhibition of CRISPR/Cas9 with NB-bearing tracrRNA and native cr-SLX4IP. The capital letter M indicates the cotreatment with *s*-TZ (512 μM), *d*-TZ (128 μM), *t*-TZ (4 μM) and *q*-TZ (4 μM). Lane 1: target control; lanes 2-3 contain native cr-SLX4IP and native tracrRNA; lanes 4-8 (*s*-TZ), 9-13 (*d*-TZ), 14-18 (*t*-TZ), 19-23 (*q*-TZ) contain native cr-SLX4IP and NB-bearing tracrRNA (a 70-min modification with 20 mM NBFI); lane 24: DNA marker.

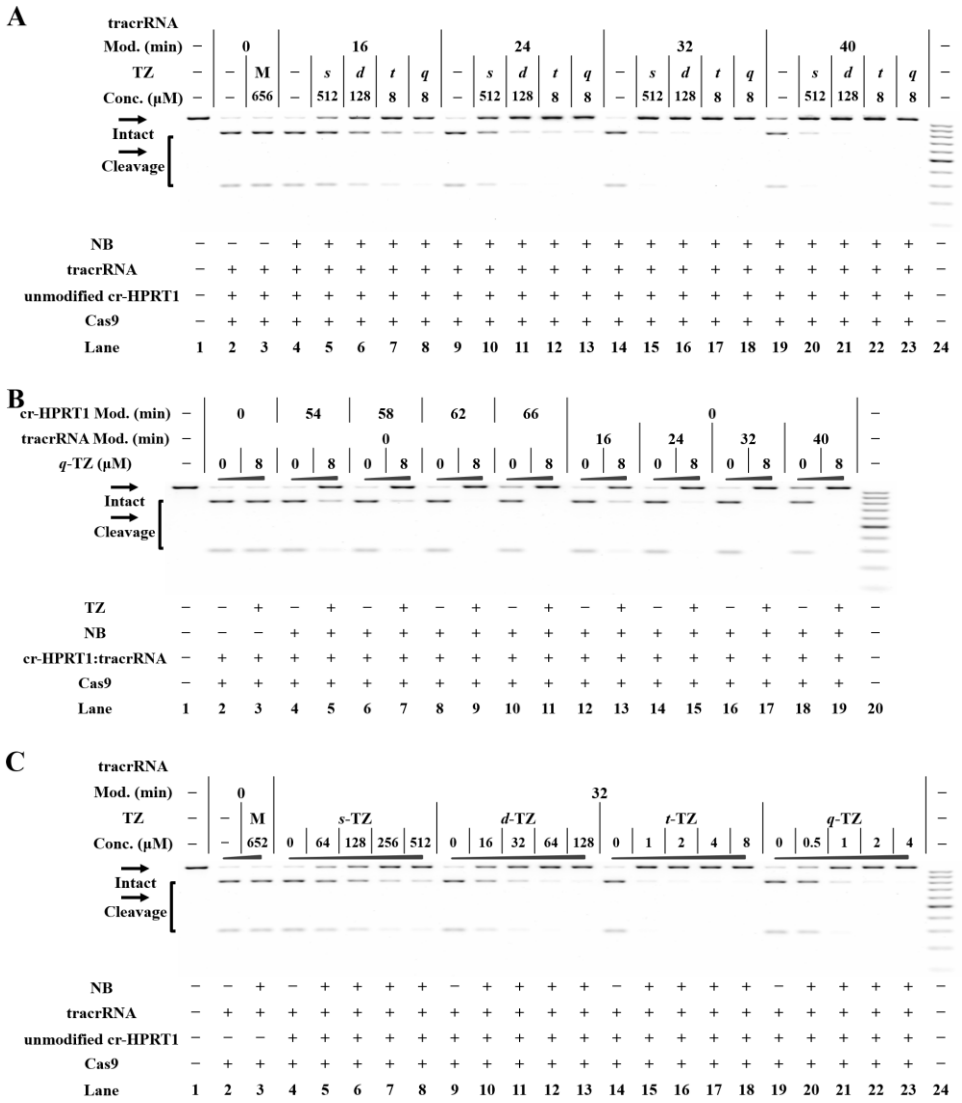

Figure S19. RNA-based NB-TZ ligation chemistry for controlling CRISPR/Cas9 with tracrRNA and cr-HPRT1.

Reactions were performed as described in the Experimental Section. For the TZ treatment, the letters *s*, *d*, *t* and *q* represent *s*-TZ, *d*-TZ, *t*-TZ and *q*-TZ, respectively. (**A**) Modification-dependent inhibition of CRISPR/Cas9 with NB-bearing tracrRNA and native cr-HPRT1. The capital letter M indicates the cotreatment with *s*-TZ (512 μM), *d*-TZ (128 μM), *t*-TZ (8 μM) and *q*-TZ (8 μM). Lane 1: no Cas9 control; lanes 2-3 contain native tracrRNA and native cr-HPRT1; lanes 4-8, 9-13, 14-18, 19-23 contain native cr-HPRT1 and NB-bearing tracrRNA with increasing modification levels; lane 24: DNA marker (GeneRuler 100-bp DNA Ladder). (**B**) Modification-dependent inhibition of CRISPR/Cas9 with *q*-TZ. In this study, either cr-HPRT1 or tracrRNA was modified with the NB moieties. Lane 1: target control; lanes 2-3 contain native cr-HPRT1 and native tracrRNA; lanes 4-5, 6-7, 8-9, 10-11 contain native tracrRNA and NB-bearing cr-HPRT1 with increasing modification levels; lanes 12-13, 14-15, 16-17, 18-19 contain native cr-HPRT1 and NB-bearing tracrRNA with increasing modification levels; lane 20: DNA marker. (**C**) Dose-dependent effect of TZ on inhibition of CRISPR/Cas9 with NB-bearing tracrRNA and native cr-HPRT1. The capital letter M indicates the cotreatment with *s*-TZ (512 μM), *d*-TZ (128 μM), *t*-TZ (8 μM) and *q*-TZ (4 μM). Lane 1: target control; lanes 2-3 contain native cr-HPRT1 and native tracrRNA; lanes 4-8 (*s*-TZ), 9-13 (*d*-TZ), 14-18 (*t*-TZ), 19-23 (*q*-TZ) contain native cr-HPRT1 and NB-bearing tracrRNA (a 32-min modification with 20 mM NBFI); lane 24: DNA marker.

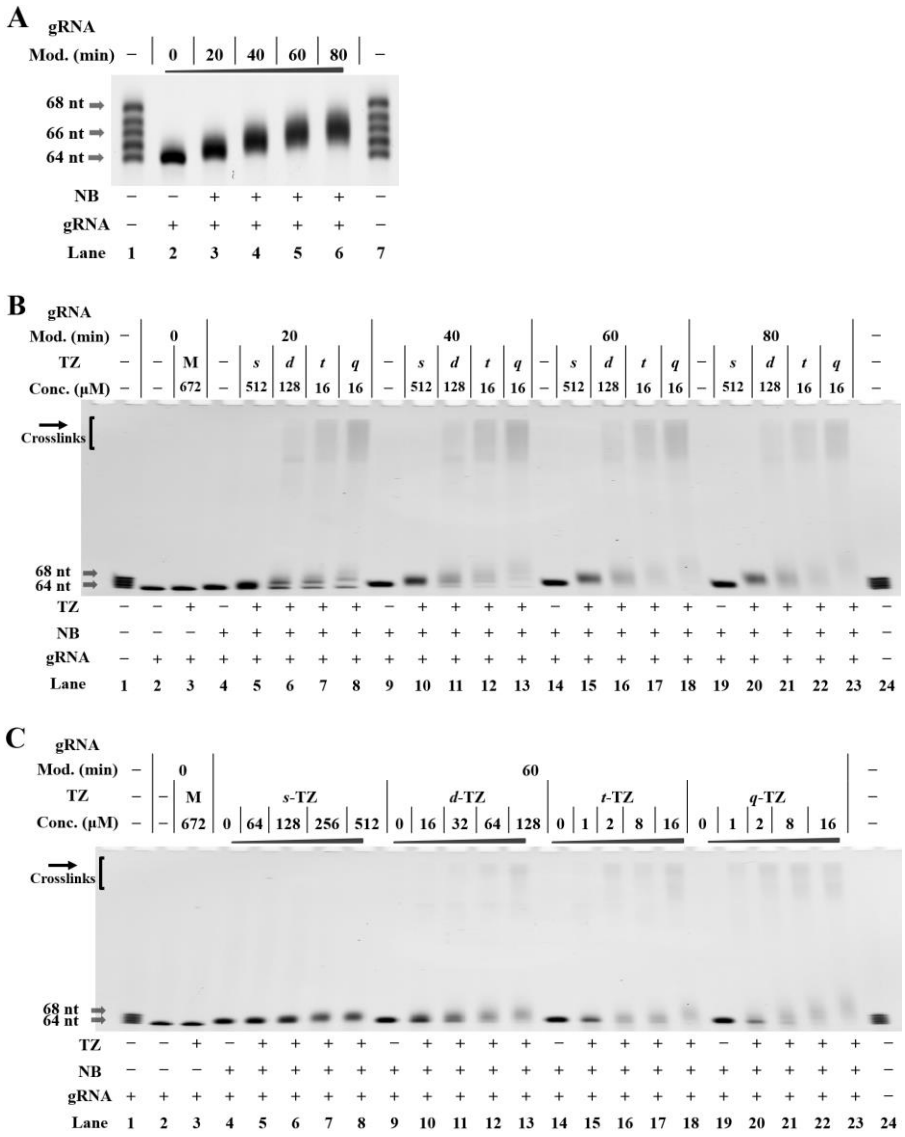

Figure S20. NB-TZ ligation chemistry with gRNA for Cas13a.

Reactions were performed as described in the Experimental Section. The treatment for each sample is indicated by the signs at the bottom of each lane. All samples were tested in three biological replicates. Image of representative data is shown here. For the TZ treatment, the capital letter M indicates the cotreatment with *s*-TZ (512 μM), *d*-TZ (128 μM), *t*-TZ (16 μM) and *q*-TZ (16 μM). (**A**) NB-functionalization of gRNA for Cas13a. Lanes 1, 7: RNA marker (R-64nt, R-65nt, R-66nt, R-67nt, R-68nt in Table S1); lane 2 contains native gRNA; lanes 3-6 contain NB-bearing gRNAs with increasing modification levels. (**B**) Modification-dependent changes in the electrophoretic mobility of NB-bearing gRNAs. For the TZ treatment, the letters *s*, *d*, *t* and *q* represent *s*-TZ, *d*-TZ, *t*-TZ and *q*-TZ, respectively. Lanes 1, 24: RNA marker (R-64nt, R-65nt, R-66nt, R-67nt, R-68nt); lanes 2-3 contain native gRNA; lanes 4-8, 9-13, 14-18, 19-23 contain NB-bearing gRNAs with increasing modification levels. (**C**) Dose response analysis of RNA retardation with NB-TZ ligation chemistry. Lanes 1, 24: RNA marker (R-64nt, R-65nt, R-66nt, R-67nt, R-68nt); lanes 2-3 contain native gRNA; lanes 4-8 (*s*-TZ), 9-13 (*d*-TZ), 14-18 (*t*-TZ), 19-23 (*q*-TZ) contain NB-bearing gRNAs with a specified level of modification (a 60-min modification with 20 mM NBFI).

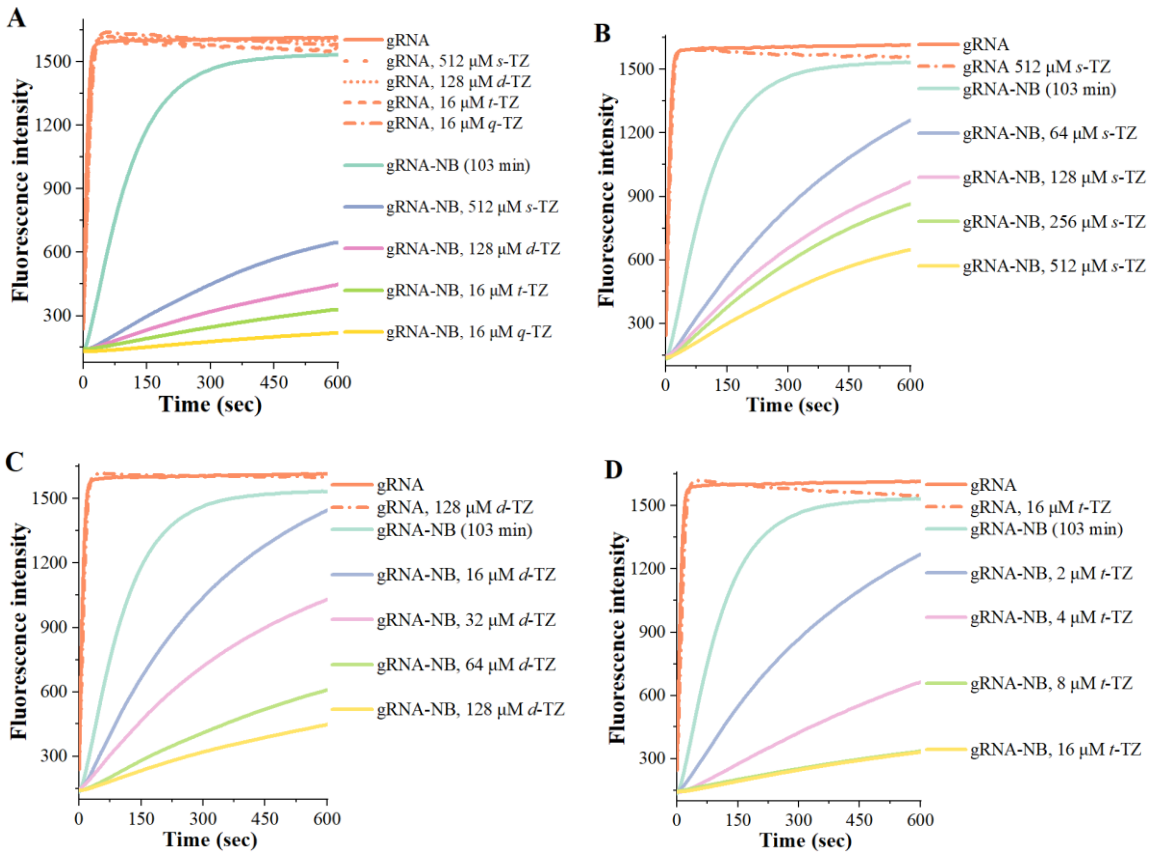

Figure S21. RNA-based NB-TZ ligation chemistry for controlling CRISPR/Cas13a.

Reactions were performed as described in the Experimental Section. NB-TZ ligation reactions were performed in the presence of all components except target RNAs. All samples were tested in three biological replicates. Image of representative data is shown here. (**A**) Effects of each TZ on the function of CRISPR/Cas13a. In this study, NB-bearing gRNAs with a specified level of modification (a 103-min modification with 20 mM NBFI) were employed to support Cas13a-mediated RNA cleavage in the absence or presence of different TZ derivatives. (**B**) Dose-dependent effect of *s*-TZ on controlling CRISPR/Cas13a. (**C**) Dose-dependent effect of *d*-TZ on controlling CRISPR/Cas13a. (**D**) Dose-dependent effect of *t*-TZ on controlling CRISPR/Cas13a. For (**B**), (**C**) and (**D**), NB-bearing gRNAs with a specified level of modification (a 103-min modification with 20 mM NBFI) were treated with increasing concentrations of each TZ.

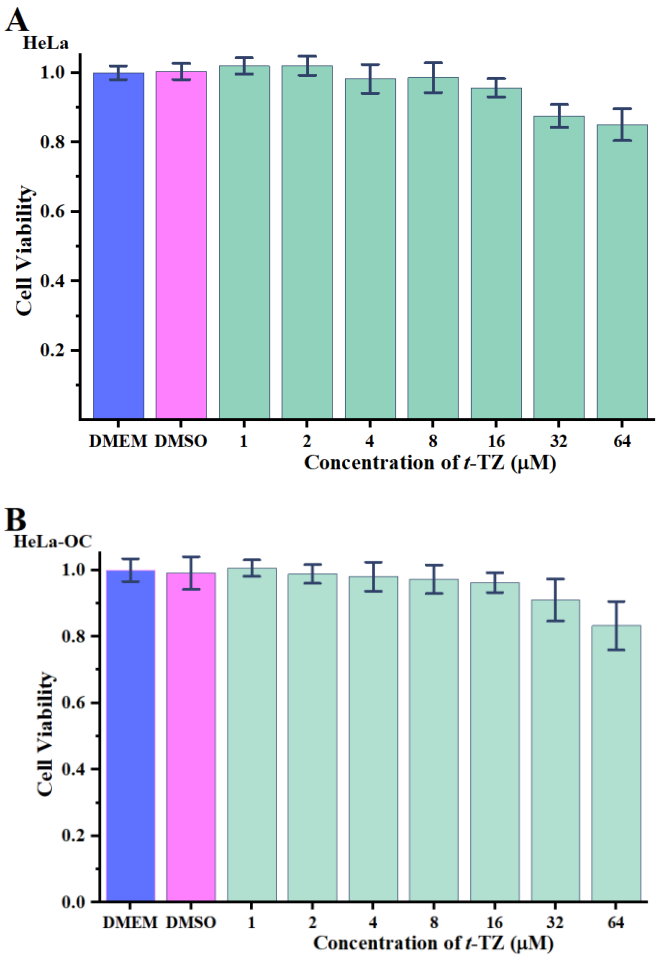

Figure S22. The cytotoxicity assay using *t*-TZ.

Cells were treated with *t*-TZ at different concentrations and toxicity was measured using the the 3-(4,5-dimethylthiazol-2-yl)-2,5-diphenyltetrazolium bromide (MTT) cytotoxicity assay. Values were plotted relative to the mean of DMEM control set to 100% (= relative growth). All data were presented as the means ± SEM from three independent experiments. Error bars: ± SEM. (**A**) Tolerance of HeLa cells to *t*-TZ. (**B**) Tolerance of HeLa-OC cells to *t*-TZ.

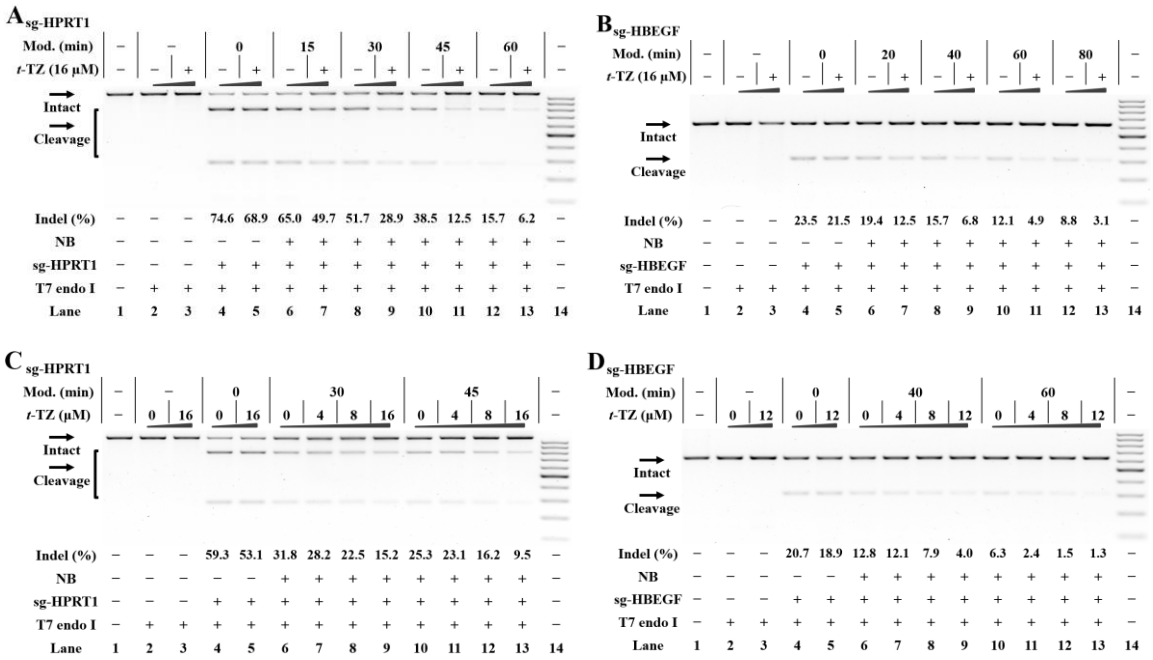

Figure S23. RNA-based NB-TZ ligation chemistry for controlling genome editing in Cas9-stable cells. Cellular studies were performed as described in the Experimental Section. Different sgRNAs were delivered into HeLa-OC cells before *t*-TZ was added. The T7E1 nuclease assay was performed 24 hr post-transfection. All samples were tested in three biological replicates. Image of representative data is shown here. (**A**) Modification-dependent inhibition of gene editing with *t*-TZ (sg-HPRT1). Lane 1: target control; lanes 2-3: no sgRNA control; lanes 4-5 contain native sg-HPRT1; lanes 6-7, 8-9, 10-11, 12-13 contain NB-bearing sg-HPRT1 with increasing modification levels; lane 14: DNA marker (GeneRuler 100-bp DNA Ladder). (**B**) Modification-dependent inhibition of gene editing with *t*-TZ (sg-HBEGF). Lane 1: target control; lanes 2-3: no sgRNA control; lanes 4-5 contain native sg-HBEGF; lanes 6-7, 8-9, 10-11, 12-13 contain NB-bearing sg-HBEGF with increasing modification levels; lane 14: DNA marker. (**C**) Dose-dependent effect of *t*-TZ on controlling gene editing (sg-HPRT1). Lane 1: target control; lanes 2-3: no sgRNA control; lanes 4-5 contain native sg-HPRT1; lanes 6-9, 10-13 contain NB-bearing sg-HPRT1 with increasing modification levels; lane 14: DNA marker. (**D**) Dose-dependent effect of *t*-TZ on controlling gene editing (sg-HBEGF). Lane 1: target control; lanes 2-3: no sgRNA control; lanes 4-5 contain native sg-HBEGF; lanes 6-9, 10-13 contain NB-bearing sg-HBEGF with increasing modification levels; lane 14: DNA marker.

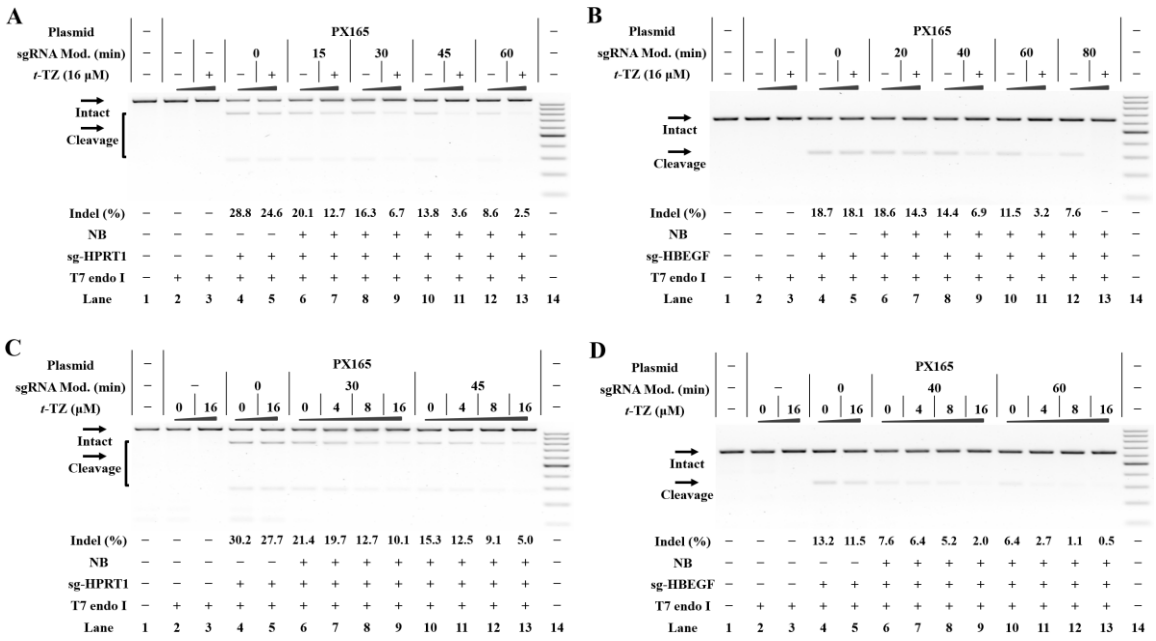

Figure S24. RNA-based NB-TZ ligation chemistry for controlling plasmid-based gene editing.

Cellular studies were performed as described in the Experimental Section. The plasmids and sgRNAs were delivered into HeLa cells before the treatment with *t*-TZ. All samples were tested in three biological replicates. Image of representative data is shown here. (**A**) Modification-response analysis of *t*-TZ on plasmid-based gene editing (sg-HPRT1). Lane 1: target control; lanes 2-3: no sgRNA control; lanes 4-5 contain PX165 and native sg-HPRT1; lanes 6-7, 8-9, 10-11, 12-13 contain PX165 and NB-bearing sg-HPRT1 with increasing modification levels; lane 14: DNA marker (GeneRuler 100-bp DNA Ladder). (**B**) Modification-response analysis of *t*-TZ on plasmid-based gene editing (sg-HBEGF). Lane 1: target control; lanes 2-3: no sgRNA control; lanes 4-5 contain PX165 and native sg-HBEGF; lanes 6-7, 8-9, 10-11, 12-13 contain PX165 and NB-bearing sg-HBEGF with increasing modification levels; lane 14: DNA marker. (**C**) Concentration-response analysis of *t*-TZ on plasmid-based gene editing (sg-HPRT1). Lane 1: target control; lanes 2-3: no sgRNA control; lanes 4-5 contain PX165 and native sg-HPRT1; lanes 6-9, 10-13 contain PX165 and NB-bearing sg-HPRT1 with increasing modification levels; lane 14: DNA marker. (**D**) Concentration-response analysis of *t*-TZ on plasmid-based gene editing (sg-HBEGF). Lane 1: target control; lanes 2-3: no sgRNA control; lanes 4-5 contain PX165 and native sg-HBEGF; lanes 6-9, 10-13 contain PX165 and NB-bearing sg-HBEGF with increasing modification levels; lane 14: DNA marker.

Table S1. DNA and RNA sequences used in the current study.

Oligomer	Sequence(from 5'to 3')	Construct
R-32nt	5'-AAGUCGAUCUCAGUGCAGUACAAGUAAUCCAU-3'	RNA
R-44nt	5'-GGGAUGCCGUUCUUCUGCUUGUGUUUUAGAGCUAUGCUGUUUUG-3'	RNA
R-64nt (Cas13a gRNA)	5'-GAUUUAGACUACCCCAAAAACGAAGGGGACUAAAACUAGAUUGCUGUUCUACCAAGUAAUCCAU-3'	RNA
R-21nt-FAM	5'-FAM-AAGCUGAUCUCGAUGACGUAC-3'	RNA
R-64nt-Cy3	5'-Cy3-GAUUUAGACUACCCCAAAAACGAAGGGGACUAAAACUAGAUUGCUGUUCUACCAAGUAAUCCAU-3'	RNA
R-21nt	5'-AAGCUGAUCUCGAUGACGUAC-3'	RNA
R-22nt	5'-AAGCUGAUCUCGAUGACGUACU-3'	RNA
R-23nt	5'-AAGCUGAUCUCGAUGACGUACUA-3'	RNA
R-24nt	5'-AAGCUGAUCUCGAUGACGUACUAC-3'	RNA
R-25nt	5'-AAGCUGAUCUCGAUGACGUACUACG-3'	RNA
R-21nt-c-FAM	5'-FAM-GUACGUCAUCGAGAUCAGCUU-3'	RNA
R-21nt-c	5'-GUACGUCAUCGAGAUCAGCUU-3'	RNA
R-102nt	5'-GGGAUGCCGUUCUUCUGCUUGUGUUUUAGAGCUAGAAAUAGCAAGUUAAAAUAAGGCUAGUCCGUUAUCAACUUGAAAAAGUGGCACCGAGUCGGUGCUUUU-3'	transcribed RNA
R-106nt	5'-GGGAUGCAUGCCGUUCUUCUGCUUGUGUUUUAGAGCUAGAAAUAGCAAGUUAAAAUAAGGCUAGUCCGUUAUCAACUUGAAAAAGUGGCACCGAGUCGGUGCUUUU-3'	transcribed RNA
R-110nt	5'-GGGAUGCAUGCAUGCCGUUCUUCUGCUUGUGUUUUAGAGCUAGAAAUAGCAAGUUAAAAUAAGGCUAGUCCGUUAUCAACUUGAAAAAGUGGCACCGAGUCGGUGCUUUU-3'	transcribed RNA
R-102nt-F	5'-TCTAATACGACTCACTATAGGGATGCCGTTCTTCTGCTTGTGTTTTAGAGCTAGAAATAGCA-3'	The forward primer for R-102nt construct
R-106nt-F	5'-TCTAATACGACTCACTATAGGGATGCATGCCGTTCTTCTGCTTGTGTTTTAGAGCTAGAAATAGCA-3'	The forward primer for R-106nt construct
R-110nt-F	5'-TCTAATACGACTCACTATAGGGATGCATGCATGCCGTTCTTCTGCTTGTGTTTTAGAGCTAGAAATAGCA-3'	The forward primer for R-110nt construct
long-R	5'-AAAAGCACCGACTCGGTGCCACTTTTTCAAGTTGATAACGGACTAGCCTTATTTTAACTTGCTATTTCTAGCTCTAAAAC-3'	The reverse primer for R-102nt, R-106nt, R-110nt construct
Pepper-F	5'-TCTAATACGACTCACTATAGGGTTGCCATGTGTATGTGGGTTCGCCCACATACTCTGATGATCCCCAATCGTGG-3'	For Pepper RNA construct

Pepper-R	5’-TTGCCATGAATGATCCCGGCGCCAGTGCCTGCCGAAGCAGGCCGACACGCCACGATTGGGGATCATCAGA-3’	
Pepper RNA	5’-GGGUUGCCAUGUGUAUGUGGGUUCGCCCACAUACUCUGAUGAUCCCCAAUCGUGGCGUGUCGGCCUGCUUCGGCAGGCACUGGCGCCGGGAUCAUUCAUGGCAA-3’	transcribed RNA
sg-SLX4IP	5’-GGGCCACAGCCAGGAUUUAAGAGUUUUAGAGCUAGAAAUAGCAAGUUAAAAUAAGGCUAGUCCGUUAUCAACUUGAAAAAGUGGCACCGAGUCGGUGCUUUU-3’	transcribed RNA
sg-HPRT1	5’-GGGCCCAAGGAAAGACUAUGAAAGUUUUAGAGCUAGAAAUAGCAAGUUAAAAUAAGGCUAGUCCGUUAUCAACUUGAAAAAGUGGCACCGAGUCGGUGCUUUU-3’	transcribed RNA
sg-HBEGF	5’-GGGUUCUCUCGGCACUGGUGACGUUUUAGAGCUAGAAAUAGCAAGUUAAAAUAAGGCUAGUCCGUUAUCAACUUGAAAAAGUGGCACCGAGUCGGUGCUUUU-3’	transcribed RNA
sg-SLX4IP-F	5’-TCTAATACGACTCACTATAGGGCCACAGCCAGGATTTAAGAGTTTTAGAGCTAGAAATAGCAAGTTAAAATA-3’	The forward primer for sg-SLX4IP construct
sg-HPRT1-F	5’-TCTAATACGACTCACTATAGGGCCCAAGGAAAGACTATGAAAGTTTTAGAGCTAGAAATAGCAAGTTAAAATA-3’	The forward primer for sg-HPRT1 construct
sg-HBEGF-F	5’-TCTAATACGACTCACTATAGGGTTCTCTCGGCACTGGTGACGTTTTAGAGCTAGAAATAGCAAGTTAAAATA-3’	The forward primer for sg-HBEGF construct
sg-R	5’-AAAAGCACCGACTCGGTGCCACTTTTTCAAGTTGATAACGGACTAGCCTTATTTTAACTTGCTATTTCTA-3’	The reverse primer for sgRNA construct
cr-SLX4IP	5’-GGGCCACAGCCAGGAUUUAAGAGUUUUAGAGCUAUGCUGUUUUG-3’	RNA
cr-HPRT1	5’-GGGCCCAAGGAAAGACUAUGAAAGUUUUAGAGCUAUGCUGUUUUG-3’	RNA
cr-HBEGF	5’-GGGUUCUCUCGGCACUGGUGACGUUUUAGAGCUAUGCUGUUUUG-3’	RNA
tracrRNA-F	5’-TCTAATACGACTCACTATAGGGTTGGAACCATTCAAAACAGCAT**A**GCAAGTTAAAATAAGGCTAG-3’	For tracrRNA construct
tracrRNA-R	5’-AAAAAAAGCACCGACTCGGTGCCACTTTTTCAAGTTGATAACGGA**C**TAGCCTTATTTTAACTTGCT-3’	
tracrRNA	5’-GGGUUGGAACCAUUCAAAACAGCAUAGCAAGUUAAAAUAAGGCUAGUCCGUUAUCAACUUGAAAAAGUGGCACCGAGUCGGUGCUUUUUUU-3’	transcribed RNA
t-SLX4IP-F	5’-TTATCC GGCACT GTG AAAGCT-3’	

t-SLX4IP-R	5’-CCTGAT GTTTAG CAAC TTTTTGG-3’	For PCR of t-SLX4IP
t-HPRT1-F	5’-GTTGTGATAAAAGGTGATGCTC-3’	For PCR of t-HPRT1
t- HPRT1-R	5’-TCATAAACACATCCATGGGAC-3’	
t-HBEGF-F	5’-GCCGCTTCGAAAGTGACTGG-3’	For PCR of t-HBEGF
t-HBEGF-R	5’-GATCCCCCAGTGCCCATCAG-3’	
R-65nt	5’-GAUUUAGACUACCCCAAAAACGAAGGGGACUAAAACUAGAUUGCUGUUCUACCAAGUAAUCCAUU-3’	RNA
R-66nt	5’-GAUUUAGACUACCCCAAAAACGAAGGGGACUAAAACUAGAUUGCUGUUCUACCAAGUAAUCCAUUA-3’	RNA
R-67nt	5’-GAUUUAGACUACCCCAAAAACGAAGGGGACUAAAACUAGAUUGCUGUUCUACCAAGUAAUCCAUUAC-3’	RNA
R-68nt	5’-GAUUUAGACUACCCCAAAAACGAAGGGGACUAAAACUAGAUUGCUGUUCUACCAAGUAAUCCAUUACG-3’	RNA
MB	5’-FAM-CGCGCTTGGTAGAACAGCAATCCGCG-Dabcyl-3’	DNA
Cas13a target	5’-UUACUUGGUAGAACAGCAAUCUA-3’	RNA
Cas13a reporter	5’-FAM-UUUUU-BHQ1-3’	RNA

Appendix A: NMR spectra copies of the selected synthesized compounds

This section contains the NMR spectra of the selected synthesized compounds. For each compound, the spectra are shown in the following order: ^{1}H NMR and ^{13}C NMR. The chemical structure of the compound is drawn on each spectrum.

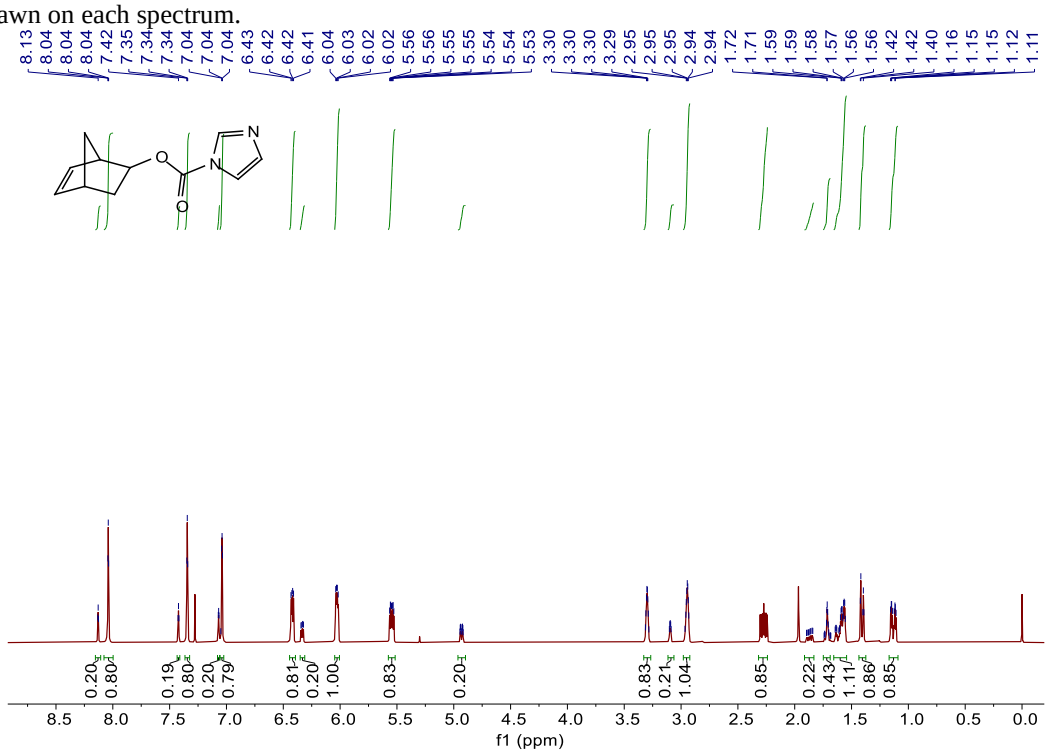

^{1}H NMR spectrum of **NBFI** in $CDCl_3$

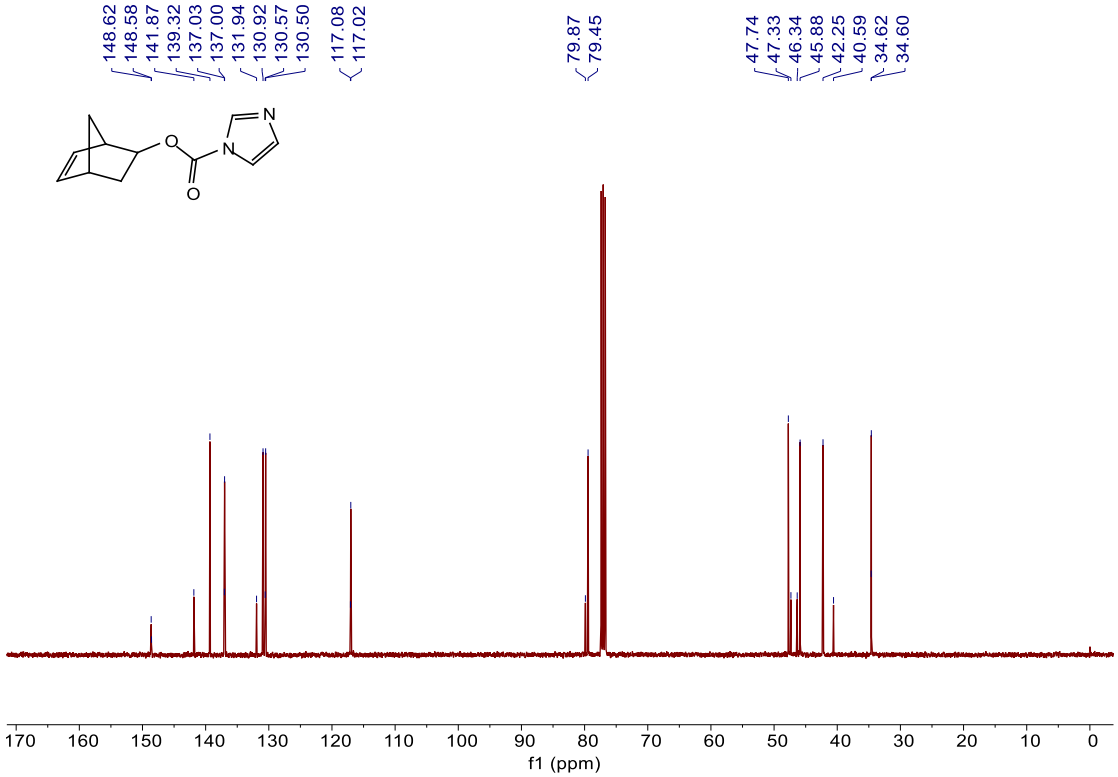

^{13}C NMR spectrum of **NBFI** in $CDCl_3$

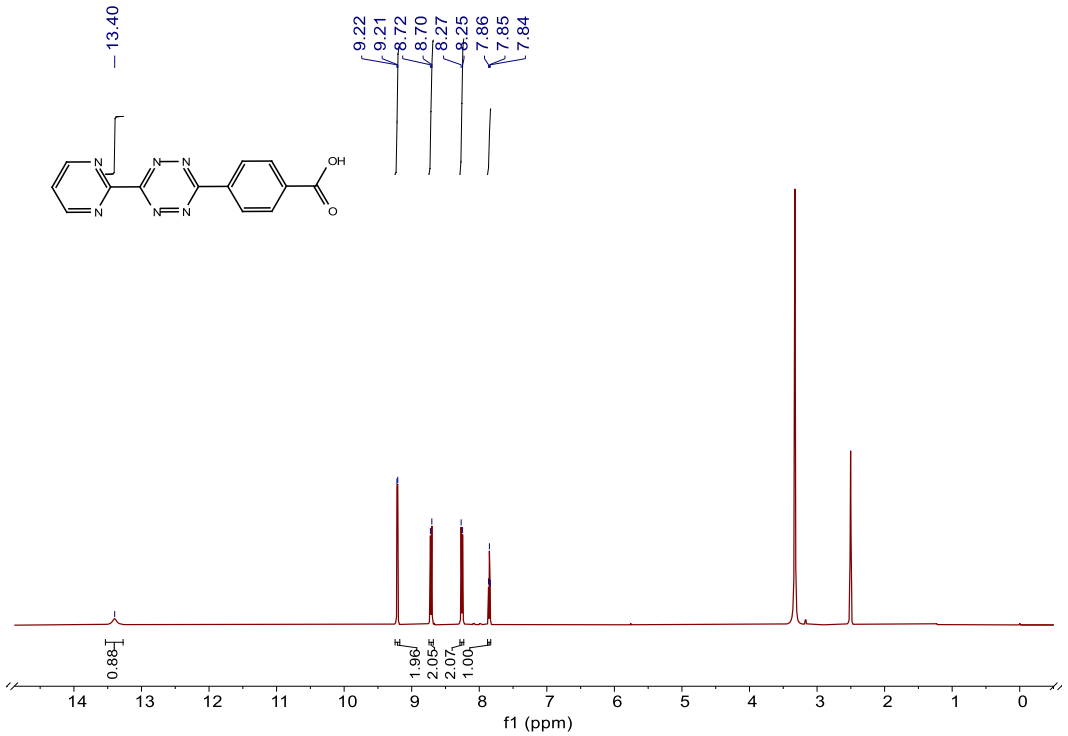

^{1}H NMR spectrum of ***s*-TZ** in $CDCl_3$

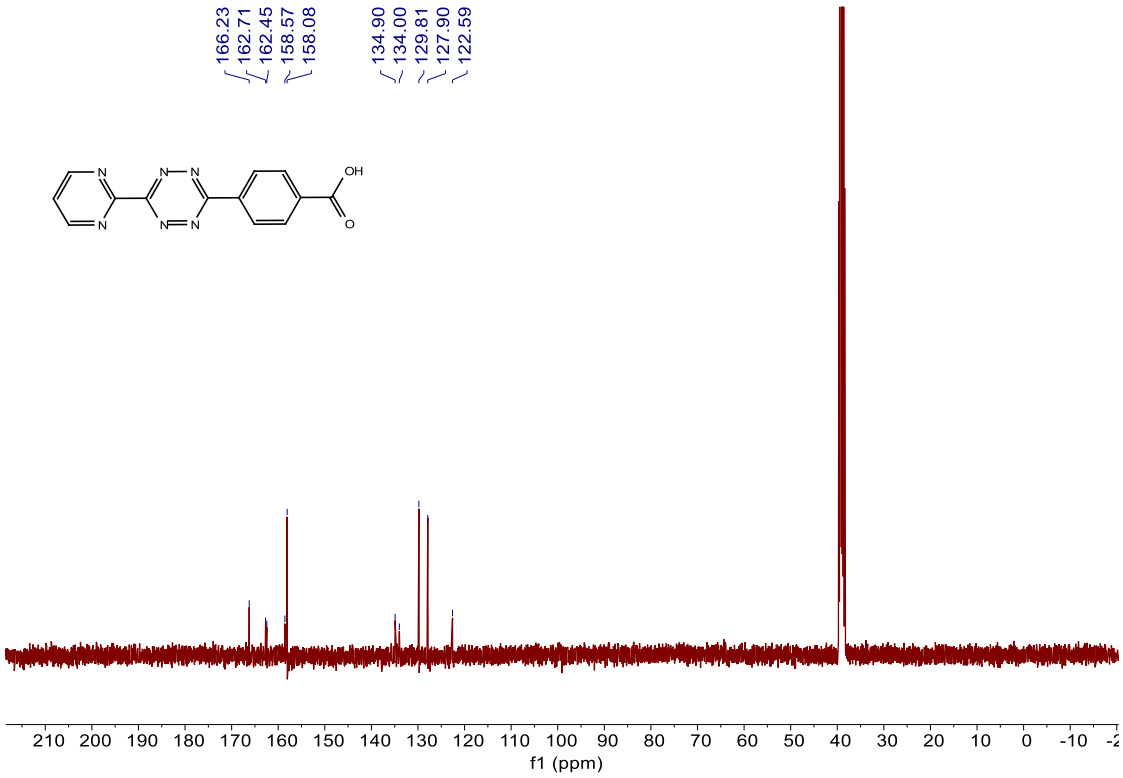

^{13}C NMR spectrum of ***s*-TZ** in $CDCl_3$

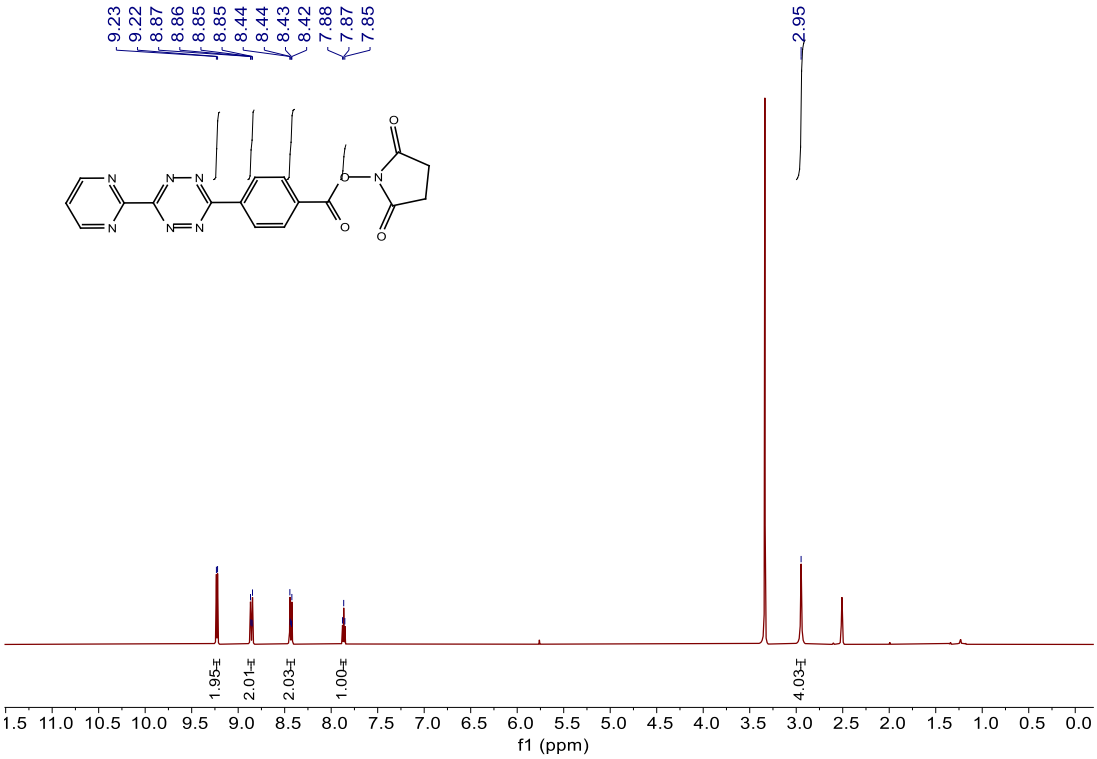

^{1}H NMR spectrum of compound **4** in $CDCl_3$

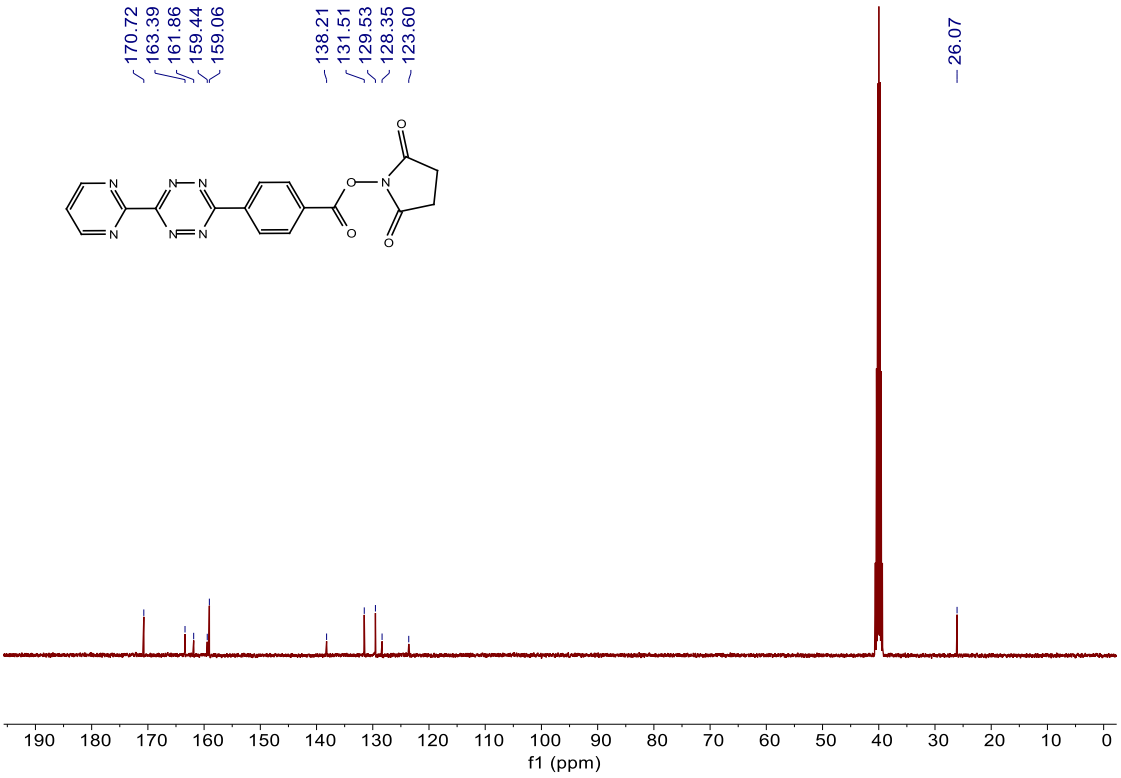

^{13}C NMR spectrum of compound **4** in $CDCl_3$

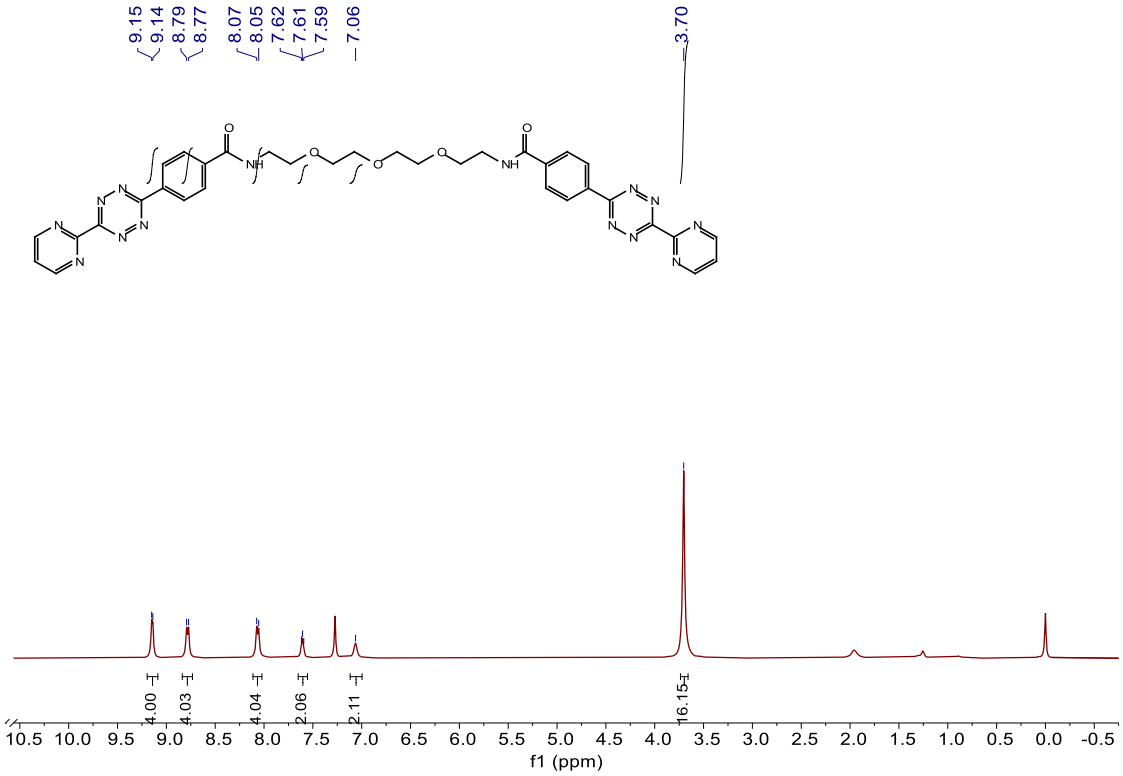

^{1}H NMR spectrum of ***d*-TZ** in $CDCl_3$

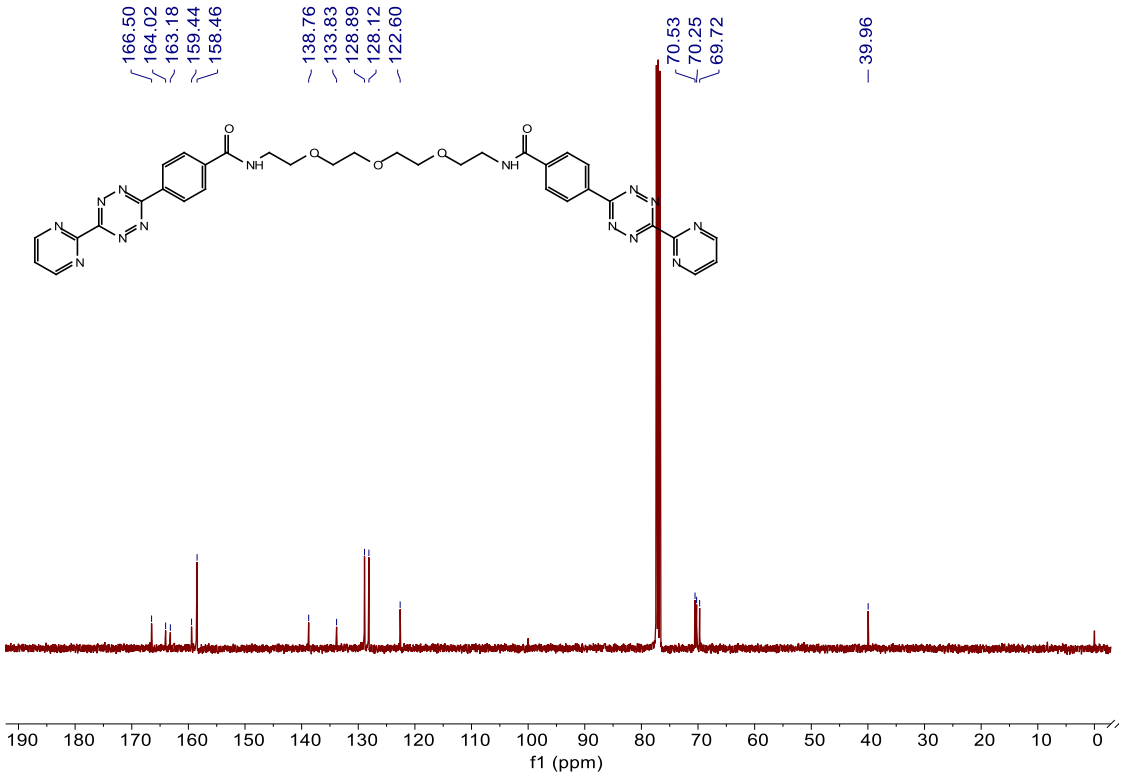

^{13}C NMR spectrum of ***d*-TZ** in $CDCl_3$

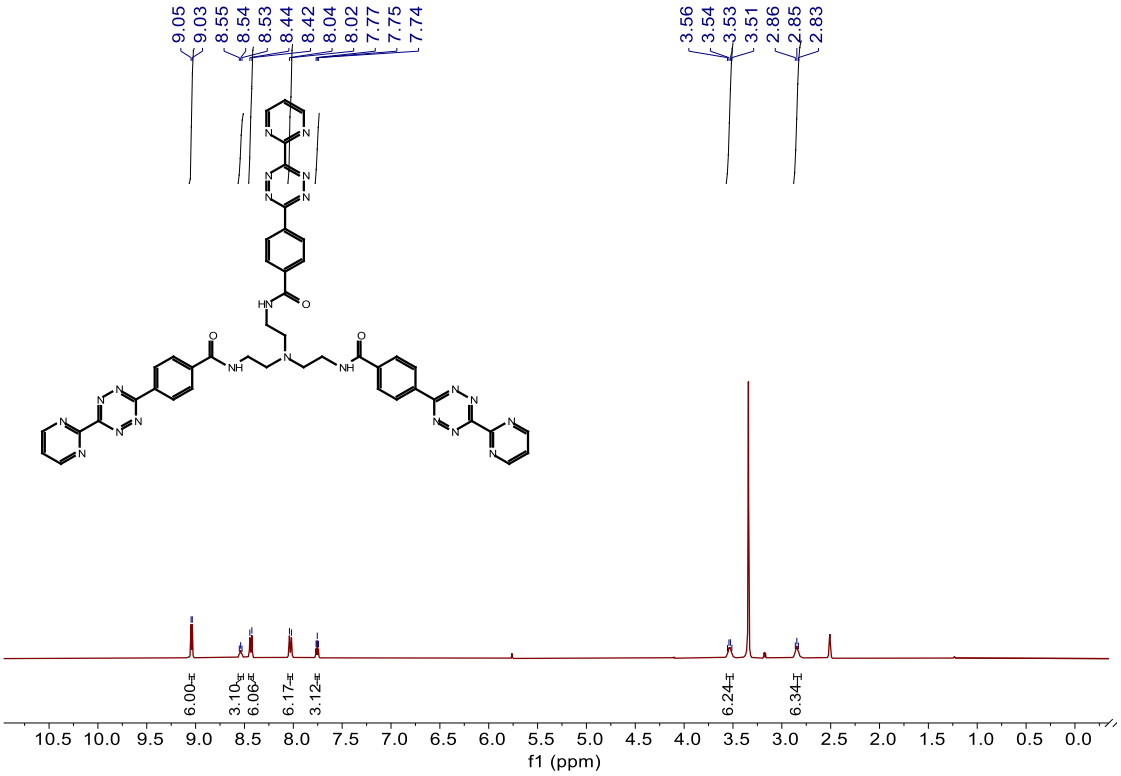

^{1}H NMR spectrum of ***t*-TZ** in $CDCl_3$

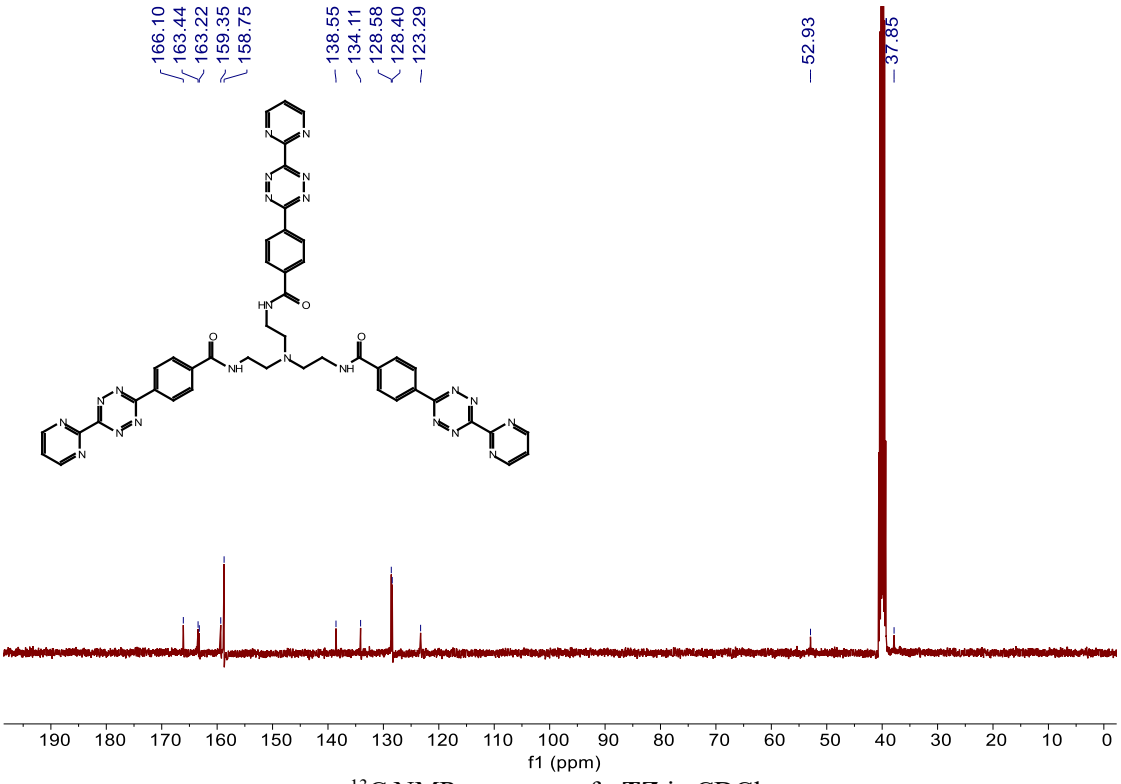

^{13}C NMR spectrum of ***t*-TZ** in $CDCl_3$

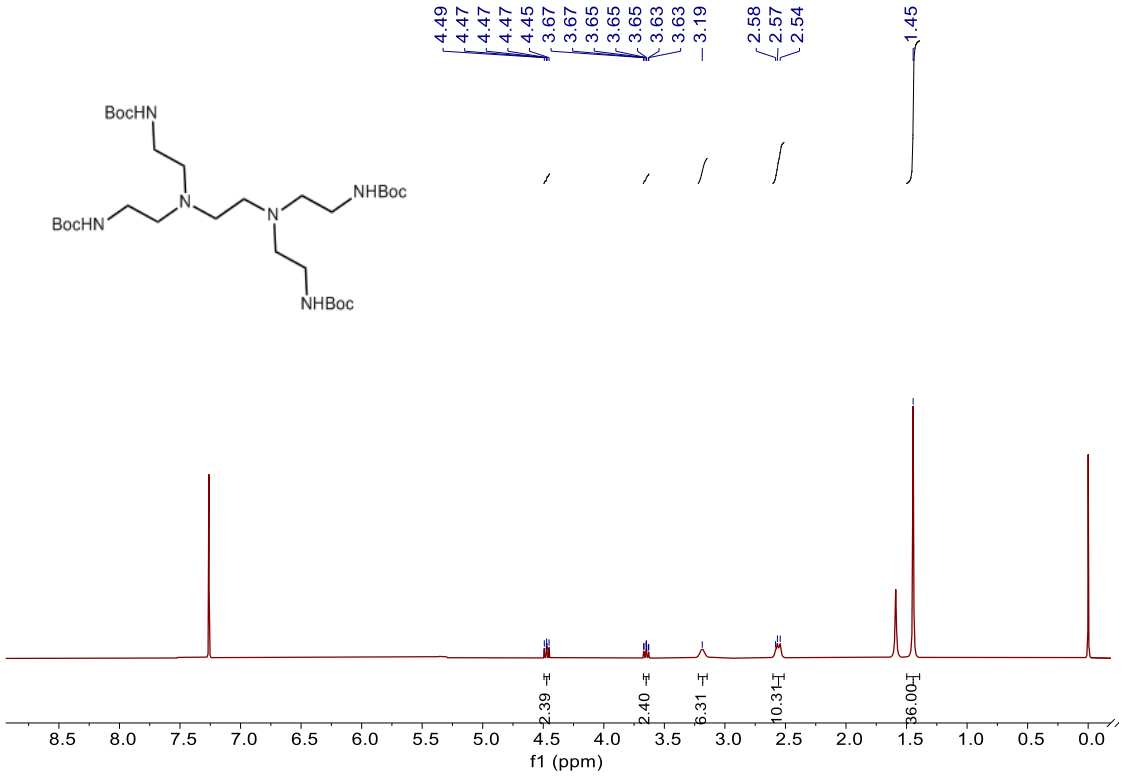

^{1}H NMR spectrum of compound **6** in $CDCl_3$

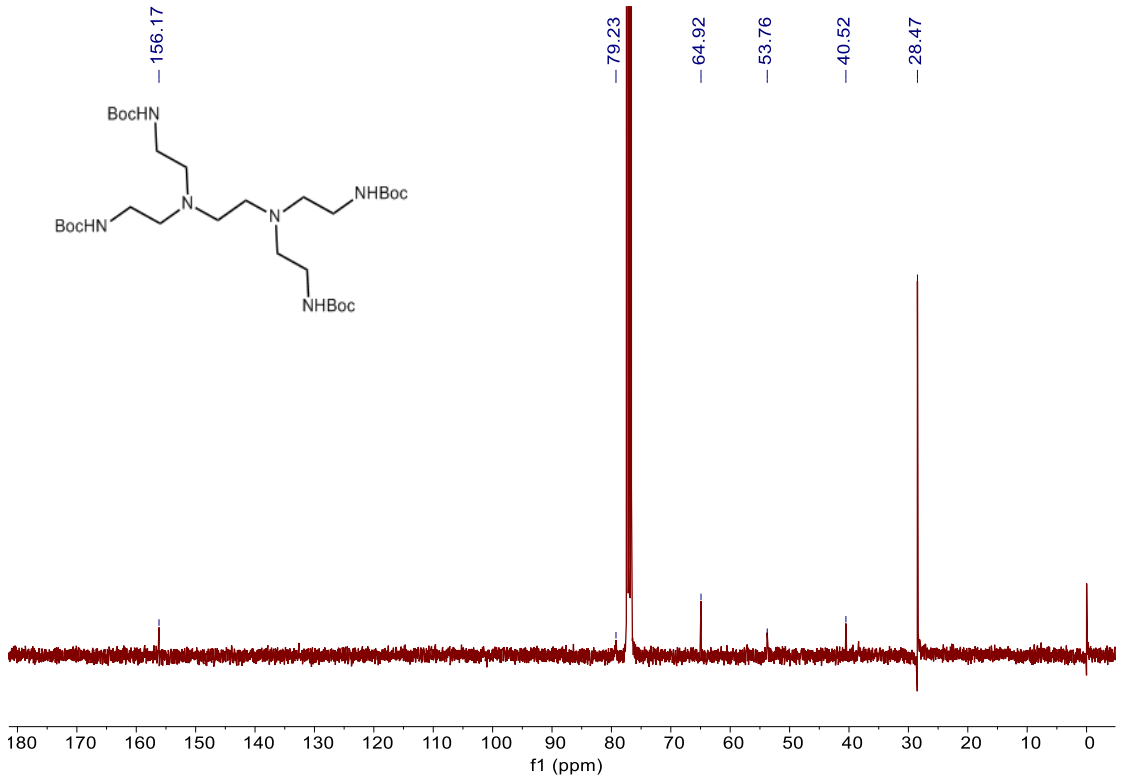

^{13}C NMR spectrum of compound **6** in $CDCl_3$

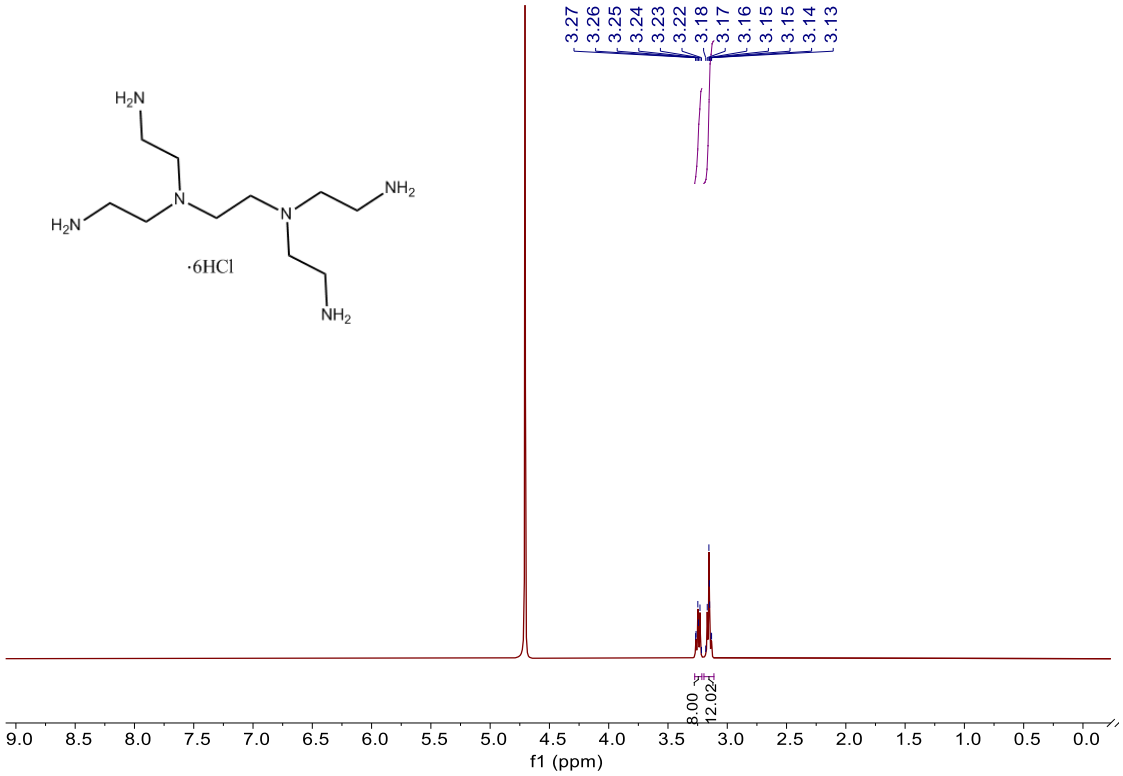

^{1}H NMR spectrum of compound **7** in $CDCl_3$

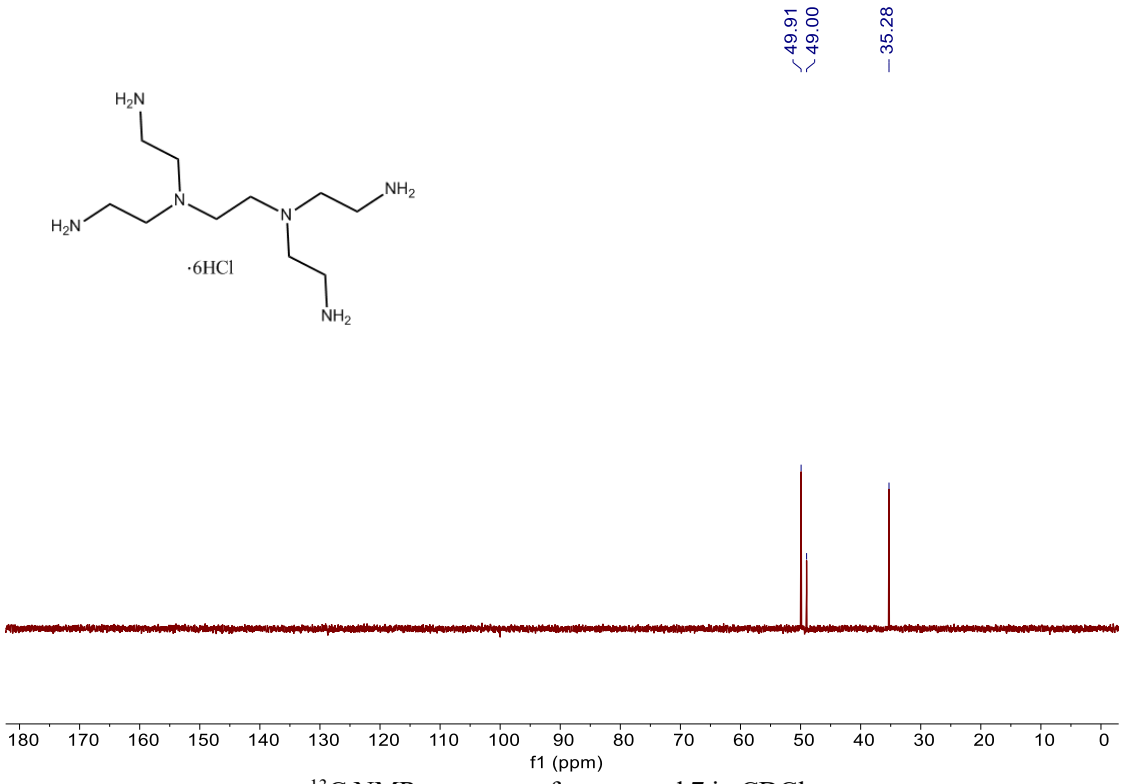

^{13}C NMR spectrum of compound **7** in $CDCl_3$

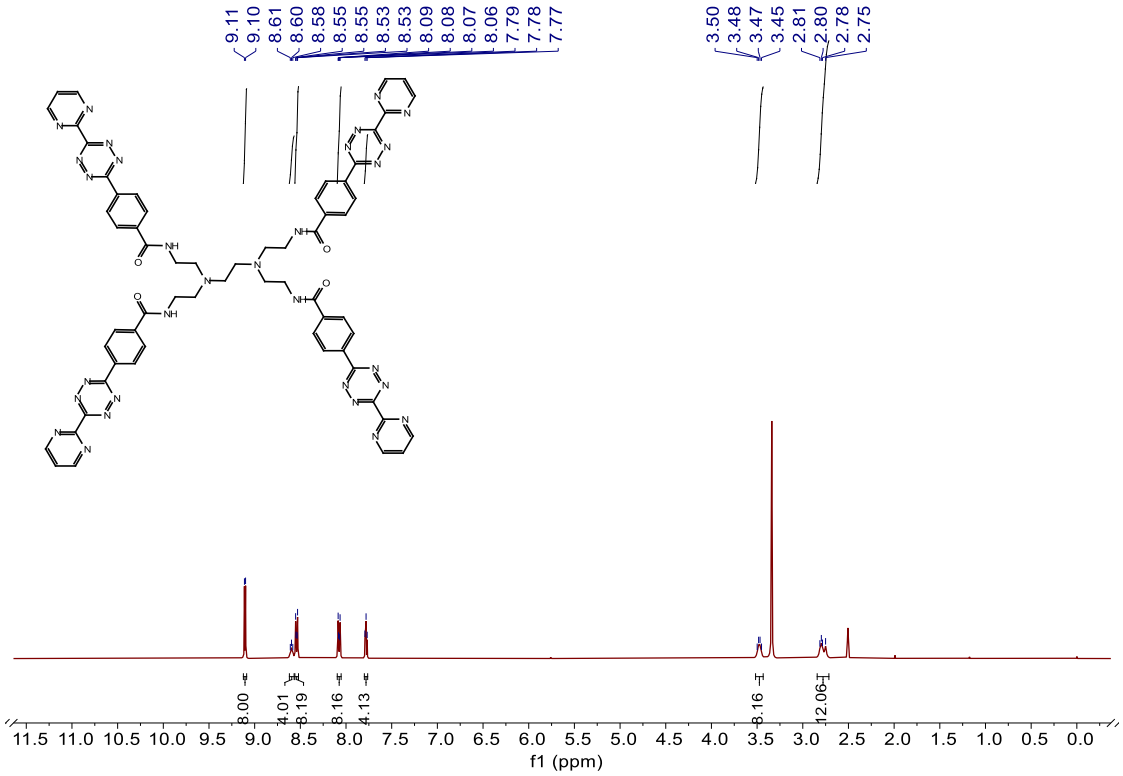

^{1}H NMR spectrum of ***q*-TZ** in $CDCl_3$

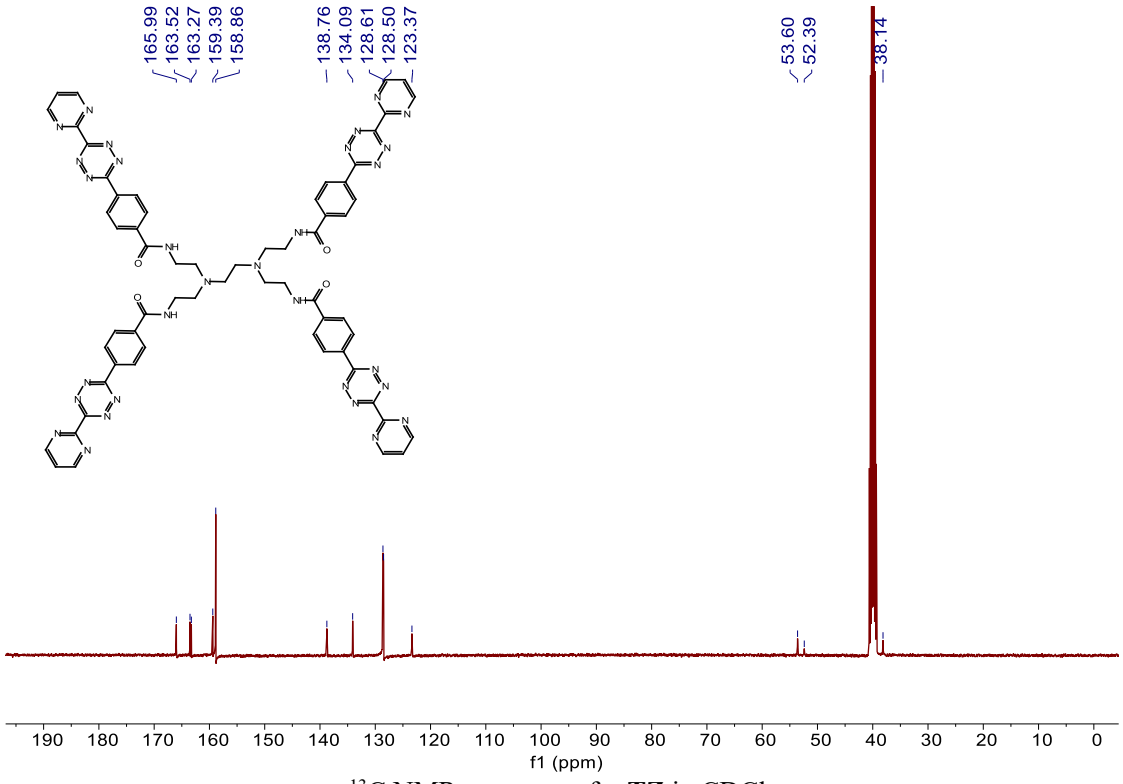

^{13}C NMR spectrum of ***q*-TZ** in $CDCl_3$

Appendix B: HRMS spectral copies of the used compounds in the current study

This section contains the HRMS spectra of the used compounds in this study. The chemical structure of the compound is drawn on each spectrum.

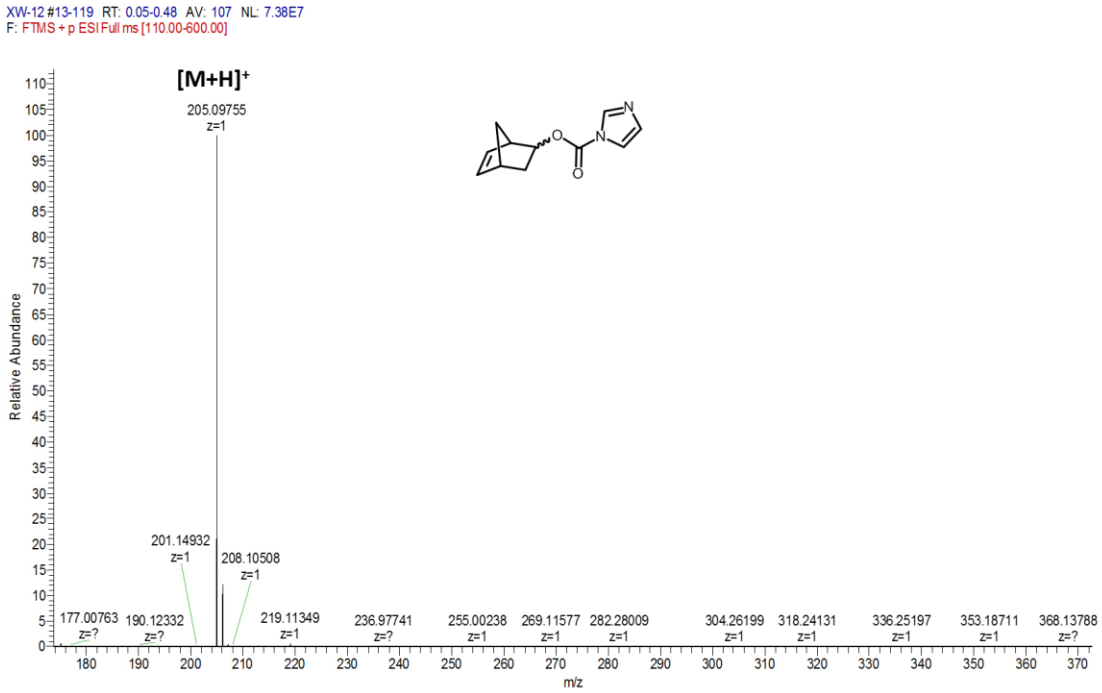

HRMS spectrum of **NBFI**

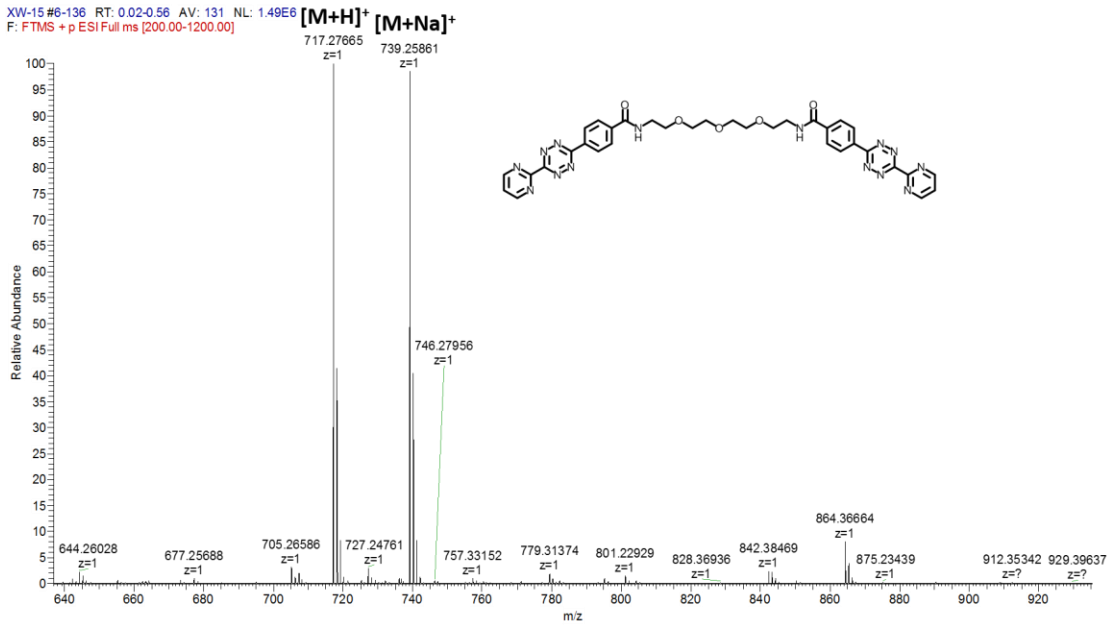

HRMS spectrum of ***d*-TZ**

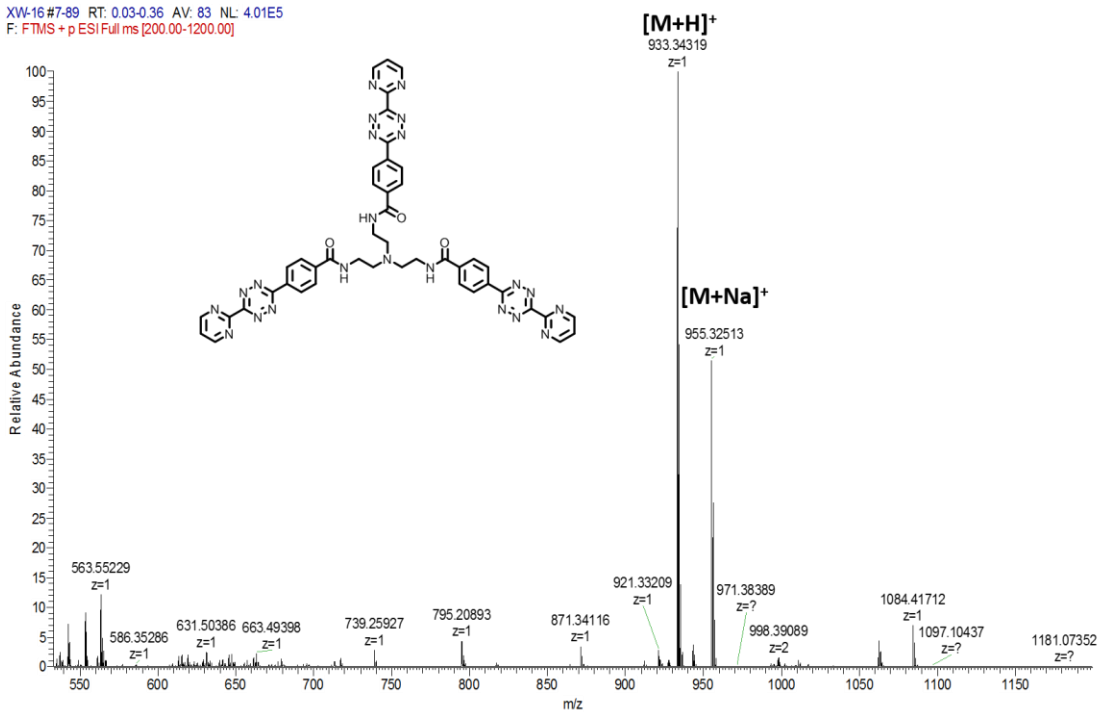

HRMS spectrum of ***t*-TZ**

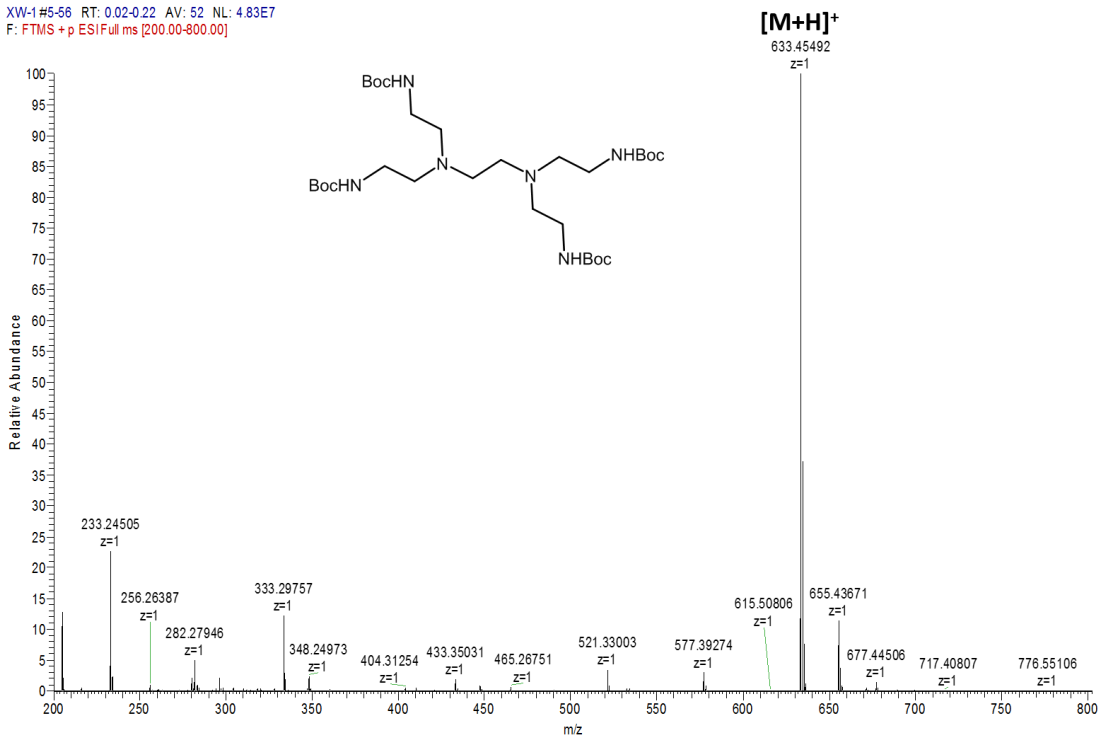

HRMS spectrum of compound **6**

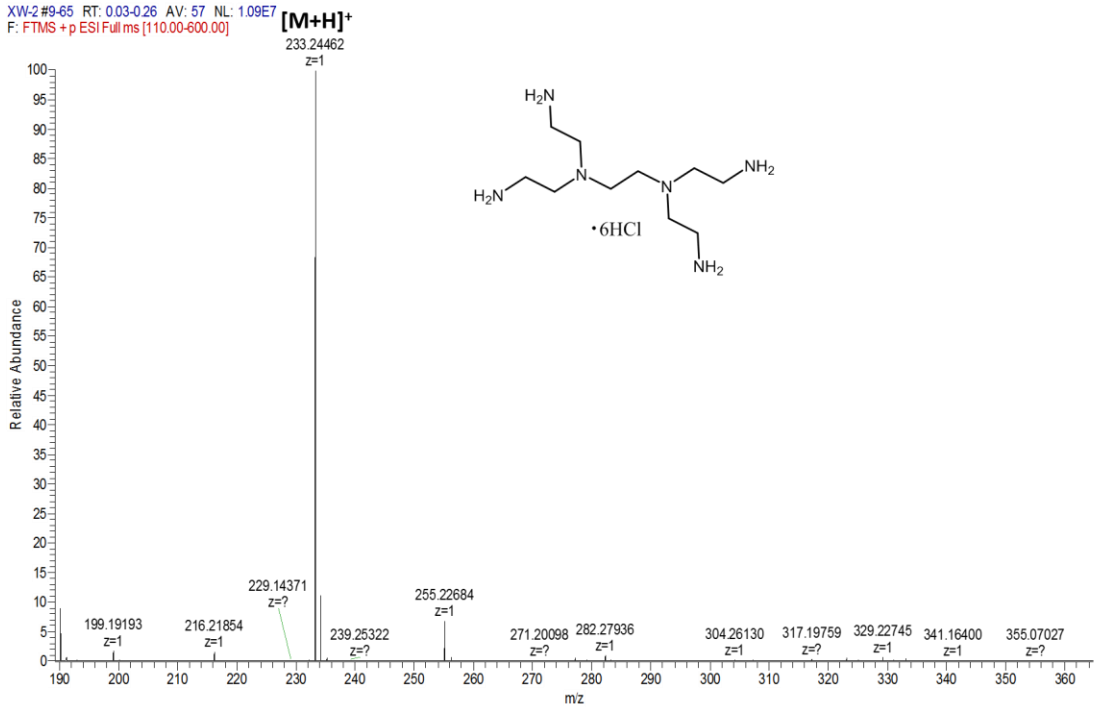

HRMS spectrum of compound **7**

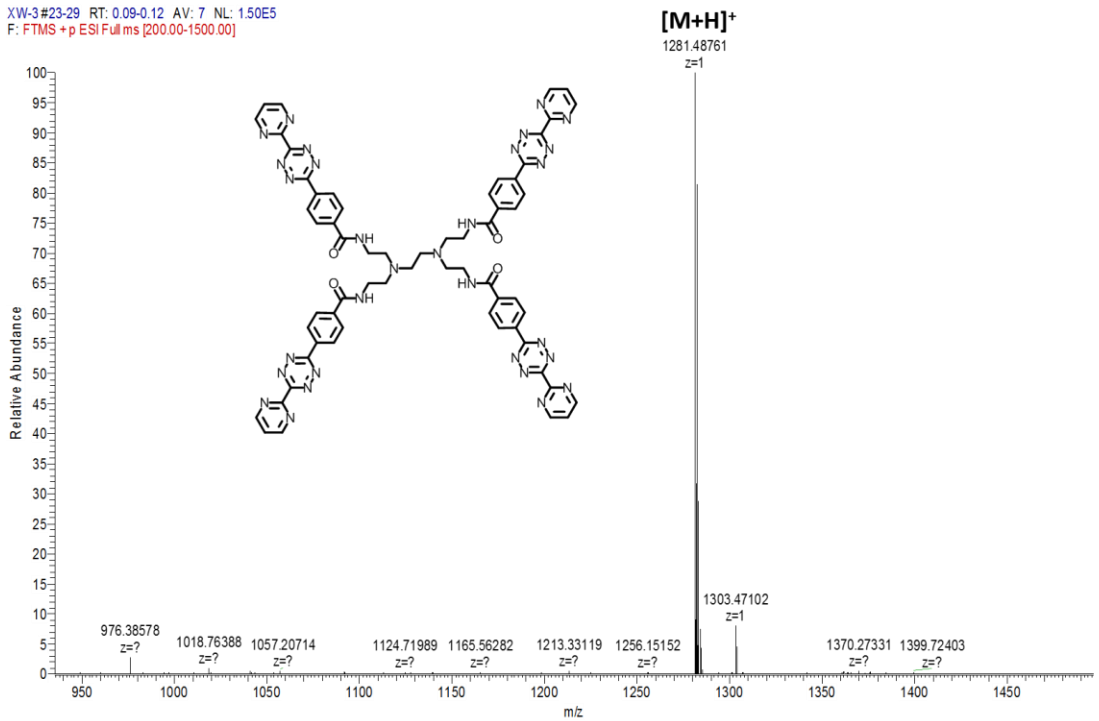

HRMS spectrum of ***q*-TZ**

SI References

1. Chen W, Wang D, Dai C, Hamelberg D, & Wang B (2012) Clicking 1,2,4,5-tetrazine and cyclooctynes with tunable reaction rates. *Chem. Commun.* 48(12):1736-1738.
2. Beckmann HSG, Niederwieser A, Wiessler M, & Wittmann V (2012) Preparation of Carbohydrate Arrays by Using Diels–Alder Reactions with Inverse Electron Demand. *Chem. Eur. J.* 18(21):6548-6554.
3. Jain PK, *et al.* (2016) Development of Light-Activated CRISPR Using Guide RNAs with Photocleavable Protectors. *Angew Chem Int Ed Engl* 55(40):12440-12444.
4. East-Seletsky A, *et al.* (2016) Two distinct RNase activities of CRISPR-C2c2 enable guide-RNA processing and RNA detection. *Nature* 538(7624):270-273.